Marine Micropaleontology 151 (2019) 101749

Contents lists available at ScienceDirect

Marine Micropaleontology

journal homepage: www.elsevier.com/locate/marmicro

Responses of benthic foraminifera to environmental variability: A case from the Middle Jurassic of the Kachchh Basin (Western India)

Sreepat Jain[a,*], Ahmed Awad Abdelhady[b], Mohamad Alhussein[c]

[a] Department of Geology, School of Applied Natural Science, Adama Science and Technology University, 1888 Adama, Oromia, Ethiopia
[b] Geology Department, Faculty of Science, Minia University, 61519 Minia, Egypt
[c] Department of Geology, Aleppo University, Aleppo, Syria

ARTICLE INFO

Keywords:
Middle Jurassic
Kachchh
Sea level
Clustering
NMDS ordination

ABSTRACT

At the western margin of the Indian plate, the Jurassic sedimentary succession of the Kachchh Basin provides well–developed exposures for fauna-based studies. Based on a quantitative analyses of 67 samples spanning Middle Bathonian–Late Callovian interval, the paleoenvironment of the Jumara section (the depocenter of the Kachchh basin), is inferred. Four benthic foraminiferal assemblages are recognized by both Clustering and NMDS ordination methods. These assemblages vary in biotic traits such as life–habit and diversity as well as in abiotic traits such as sediment type, nutrient availability, and oxygen level. The Bathonian *Spirillina polygyrata* assemblage that dominates an outer neritic oligotrophic setting, has a preference for calcareous substrates. In the earliest Callovian, the *Epistomina mosquensis* assemblage replaced the latter, as oxic conditions decreased and terrigenous influx increased. Two successive and less diverse assemblages had a preference for non–calcareous substrates and dominated the mid-Early–Late Callovian landscape. These are the oxic *Lenticulina subalata* assemblage (inner to middle neritic oligotrophic setting) in the mid–Early to mid–Middle Callovian and the dysoxic *Reophax metensis* assemblage (mesotrophic to eutrophic middle neritic setting) in the late–Middle to Late Callovian. Linear regression models suggested that sea level, oxygenation, and sediment type are the main abiotic factors controlling the distribution of the fauna. Moreover, taxa with specific biotic traits such as shell composition (calcareous vs agglutinated), and selection strategy (r vs k strategy) occupied different environmental settings. Furthermore, diversity and epifaunal/infaunal ratio had a cyclic pattern, comparable to those of third order sea–level fluctuations.

1. Introduction

The benthic invertebrates are valuable tools for paleoenvironmental reconstructions (e.g. Fürsich and Werner, 1986; Abdelhady and Mohamed, 2017). Although there are many environmental variables, quantitative models may provide plausible interpretations based on community ecology instead of using single taxon approach (Abdelhady and Fürsich, 2014). The abundance patterns of benthic foraminifera are excellent sensitive indicators for accessing changes in both paleoenvironment and bathymetry and, thus, have been extensively used to better understand the prevailing benthic environment. In the Jurassic, several studies have used the distribution of foraminifers to infer and access varied biotic and abiotic parameters. They have been used to interpret bottom water oxygen levels (Kaminski et al., 1995), trophic conditions (Reolid et al., 2008a), the interrelationship between the composition of foraminiferal assemblages, lithofacies, and paleogeography (Olóriz et al., 2002, 2003), sea level fluctuations (Hughes, 2004), palaeoclimate (Gómez et al., 2009), palaeoproductivity and redox conditions (Reolid and Martínez-Ruiz, 2012), and paleobiogeography (Kottachchi et al., 2002). In addition, the test shape (= morphogroups) has also been utilized to infer changes in the paleoenvironment (Nagy et al., 1995; Reolid et al., 2008b).

The use of multivariate analysis to infer paleoenvironmental and paleoecological changes have added more value to the study of benthic formainifera as a proxy for inferring the paleoenvironment and bathymetry (Canales Fernández et al., 2014). The Kachchh Basin (Western India; Fig. 1), due to its great diversity of facies and benthic fauna, provides an excellent opportunity to quantitatively test the robustness of benthic foraminiferal distribution patterns vis–à–vis basinal dynamics. Thus, the aim of the present contribution is to use the foraminiferal data from the Jumara Dome, the depocenter of the Kachchh Basin (Fig. 1), to quantitatively address the following hypotheses:

* Corresponding author.
E-mail address: sreepatjain@gmail.com (S. Jain).

https://doi.org/10.1016/j.marmicro.2019.101749
Received 22 March 2019; Received in revised form 12 June 2019; Accepted 20 June 2019
Available online 02 July 2019
0377-8398/ © 2019 Elsevier B.V. All rights reserved.

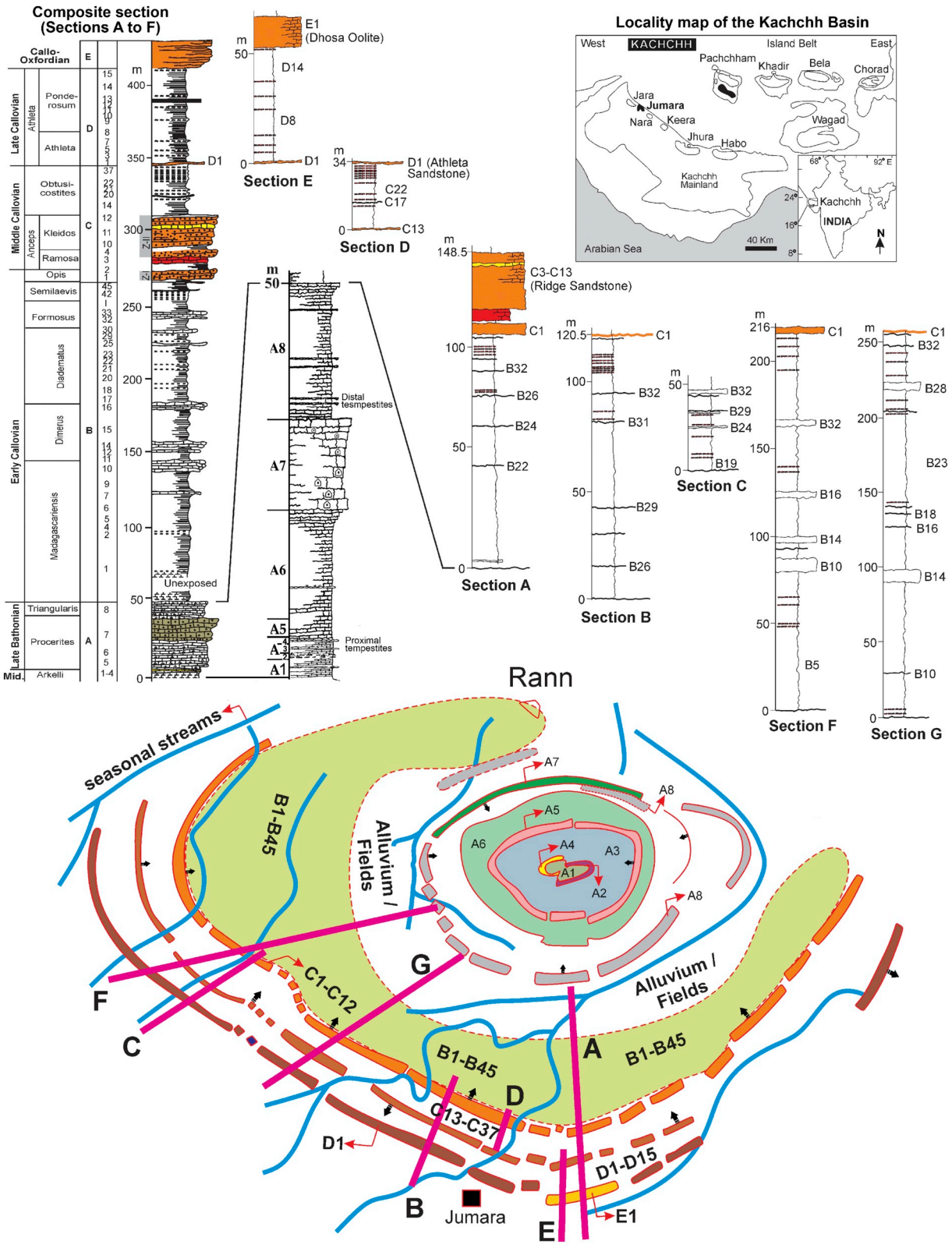

Fig. 1. Profile section of the Jumara Dome and the seven traverses (A to G) used for constructing the composite section. Inset: Locality map of the Kachchh Basin showing the location of the study area, Jumara Dome (after Jain, 1996, 2014).

1) Can biotic traits (life–habit, species diversity and shell composition: agglutinated vs. calcareous) be correlated to specific abiotic factors (sea level, sediment type, and oxygen level)?

2) What are the main factors controlling the distribution pattern of the benthic foraminifera?

Though, Kachchh Basin macrofauna and facies have been investigated earlier (Fürsich et al., 1991, 1992, 2004; Fürsich and Pandey, 2003), but the distribution patterns of benthic foraminifera have not yet been fully investigated. Those that have been done, are largely restricted to documenting basic taxonomy, or inferring broad

paleoenvironmental basinal conditions (open marine or restricted / deep or shallow basin settings) (e.g., Bhalla and Abbas, 1978; Bhalla and Talib, 1991; Pandey and Dave, 1993; Talib and Gaur, 2005; Gaur and Talib, 2009). Although an attempt was made to integrate foraminifera–ammonite data by Krishna and Ojha (2000), the base foraminiferal dataset suffers from erroneous biostratigraphy (see Jain and Pandey, 2000) and benthic foraminiferal zonation, which at places, has suspect taxonomy; well–addressed by Alhussein (2010, 2014). Additionally, the relative sea level curve for the Kachchh Basin has only been attempted on a broader scale using either the distribution of shell concentrations (transgressive lags or shell beds) (Fürsich and Oschmann, 1993) or using low resolution stable isotopes of carbon and oxygen, with clay mineralogical data (smectite, kaolinite and illite abundances; Fürsich et al., 2005). Hence, a more comprehensive approach with robust quantitative analyses is urgently warranted to better document benthic foraminiferal responses to climatic changes; this is attempted here. The contribution attempts to document benthic foraminiferal responses to the already-known basinal climatic fluctuations (regional) and not in the global climate context (as the latter would necessitate a much higher resolution sampling. However, inferences vis-à-vis with global sea level (Haq, 2018) is attempted.

2. Geological setting

The evolution of the western continental–margin basins of India is related to the breakup of the Gondwana in the Triassic/Jurassic and the subsequent spreading history of the Indian Ocean, resulting into a series of regional and local horsts and grabens (Biswas, 1991). The rifting led to the depression and the subsequent formation of rift valleys oriented East-West. The Kachchh rift basin is located at the western continental margin of India, which was inundated in the Pliensbachian-Toarcian (Early Jurassic; Rai and Jain, 2013) that resulted in the deposition of > 2000–3000 m thick Mesozoic and Cenozoic sedimentary succession (Biswas, 1991). The Jumara Dome (Kachchh Basin; Fig. 1), exposes 420 m thick Middle Jurassic (Middle Bathonian to Late Callovian; the study interval) sediments; these are also one of the thickest sequences of this time span for the *peri*–Gondwana margin with abundant benthic and nektic fauna (Jain et al., 1996; Fürsich et al., 2001, 2013). These, thus, provide an excellent opportunity to better understand the depositional history of the basin. Additionally, the latitudinal location of the Kachchh Basin is also a key to better understand not only the evolution of the Malagassy Gulf, but also of the opening of the Arabian Sea and that of the western Indian Ocean, at large.

The details of the study area, Jumara Dome (Fig. 1; inset) are given in Table 1, along with the data used in this study. The ammonite biostratigraphy used in this study is after Jain (1996, 2014) with 12 zones and 4 subzone (Fig. 2) and have been identified based on the presence of index forms coeval with those occurring within the Submediterranean and European standard zones and abundance patterns. A more detailed ammonite biozonation will be published elsewhere.

3. Materials and methods

Sixty–seven samples were analyzed from the Jumara section north of Kachchh Basin (N23°41′, E69°04′; see Fig. 3 and Table 1). These samples were then disaggregated using 10% hydrogen peroxide and washed through 63 μm, 125 μm, 250 μm and 500 μm mesh sieves. After drying the residue, the samples were divided into four fractions: < 63 μm, 63–125 μm, 125–250 μm, 250–500 μm and > 500 μm. The foraminifers were picked from 200 g of the samples from the > 125 μm fraction (Alhussein, 2010, 2014). The 67 benthic foraminiferal samples were placed (as precisely as possible) within the updated ammonite biozones of the section (see Jain, 1996, 2014, Jain and Pandey, 2000; Fig. 2).

Q–mode cluster analysis of the species–abundance dataset was used to identify benthic foraminiferal associations. The dendrogram of the cluster has been constructed based on Ward's method. The strength of the clustering was checked by the cophenetic correlation coefficient (CCC; a measure of how a dendrogram preserves the pairwise distances between the original data points; Abdelhady and Fürsich, 2014). Moreover, the species/samples matrix has been examined with Non–-Metric Multidimensional Scaling (NMDS) and the goodness of fit was assessed for stress value (for details see Abdelhady and Fürsich, 2015). For the community ecology analysis, the trophic nucleus (i.e. those taxa that contribute 80% of the total specimen number per association) was used (see Neyman, 1967; Abdelhady and Fürsich, 2014). The Bathonian–Callovian sea–level data (Haq, 2018) was integrated with the benthic foraminiferal occurrence data matrix (see Table 1). The Benthic Foraminiferal Oxygen Index (BFOI) of Kaiho (1991) was used to access paleoxygenation of bottom waters. The index is based on the categorization of benthic foraminifers into three groups, Oxic (O), Suboxic (S) and Dysoxic (D); BFOI is defined as [O/(O + D) x 100], where O is the number of oxic species and D the number of dysoxic species. When O = 0 and D + S > 0 (S is the number of suboxic indicators), then the BFOI value is given by [(S/(S + D)–1] x 100 (Fig. 3 and Table 2).

The bathymetric zonation used here is after Leckie and Olson (2003): Inner neritic (0–50 m), middle neritic (50–100 m), outer neritic (100–150 m) and upper bathyal (> 150 m). In addition, sediment type (calcareous vs non–calcareous), fauna life–mode (i.e. epifaunal vs infauna), BFOI, and shell composition (i.e. agglutinated vs calcareous), were also integrated in the quantitative analysis (see Table 1). To resolve the effect of the multicollinearity and the heteroscedasticity of the data, the Euclidean norm transformation was applied to all variables before applying the statistical analyses (Theodoridis and Koutroumbas, 2008).

Pearson correlation and Reduced Major Axis (RMA) linear regression model were used to assess the relationship between the fauna and the biotic/abiotic traits. In addition, we tested the significance for all determined correlations at the significance level ($p < .001$) using a one–tailed t–test. Species diversity (Shannon and Dominance; see Fig. 3) was also calculated for each sample. All statistical analyses were carried out using PAST V. 2.17c (http://folk.uio.no/ohammer/past/; Hammer et al., 2001).

Based on field and lithological observations, parasequences (coarsening upward cycles) were reconstructed and coupled with the above mentioned biotic and abiotic parameters, a relative sea level curve was constructed (Fig. 4). Furthermore, previously published data are integrated. These include data on clay mineralogy, faunal content (largely the distribution of bivalves, corals and sponges), trace fossils, shell concentrations (or shell beds), occurrence of bored concretions, and stable isotopes of carbon and oxygen in a framework of new and high–resolution stratigraphy, marked by well–calibrated age–diagnostic ammonite content (Fig. 2).

4. Results

4.1. Statistical analyses

For each sample, the BFOI, epifaunal/infaunal percentage, agglutinated/calcareous percentage, species richness, Shannon, and Dominance were calculated. The results show marked temporal variations. Both diversity and epifauna/infauna show a clear meter–scale cyclicty (Fig. 3) suggesting a possible relation to sea–level. Based on Clustering, four assemblages are recognized (Fig. 5). These assemblages (illustrated in Figs. 6–7) were named after the most dominant species, 1) *Spirillina polygyrata*, 2) *Lenticulina subalata*, 3) *Epistomina mosquensis,* and 4) *Reophax metensis.* These assemblages vary in biotic traits such as life–habit and diversity as well as in abiotic traits such as sediment type and oxygen level (Table 3).

The NMDS ordination plot based on the abundances of benthic foraminifera species also retains a clear separation between the four identified associations, where the samples were loaded on the NMDS

Table 1
Data used in the present study (see text for explanation).

Age		Ammonite bed nos (Fig. 1)		Thickness (m)	GPS location	Foram sample nos. (this study)	total benthic count	Sediment type	% Epifaunal	% Infaunal	Reophax
Callovian	Late	D	D1-D15	74	N23°40′55.6″, E69°03′47.6″	67	8541	Silt	20.3	79.7	2064
						66	12,867	Silt	0.0	100.0	1951
						65	10,000	Silt	53.5	46.5	3023
						64	8285	Silt	35.3	64.7	3415
						63	8709	Silt	24.4	75.6	2581
						62	9444	Silt	19.9	80.1	1736
	Middle	C	C1-C37	68	N23°41′02.1″, E69°03′46.6″	61	8806	Silt	50.9	49.1	2388
						60	10,000	Silt	6.7	93.3	2239
						59	10,000	Silt	50.8	49.2	1832
						58	5405	Sandy silt	14.7	85.3	0
						57	9142	Silty-clay	91.0	9.0	3071
						56	10,000	Silty-clay	75.0	25.0	1676
						55	9781	Silty-clay	86.7	13.3	753
						54	10,000	Silty-clay	14.4	85.7	2213
						53	9590	Silty-clay	11.2	83.6	2328
						52	10,000	Silty-clay	2.4	97.6	3016
						51	10,000	Silty-clay	45.0	55.0	2852
						50	10,000	Silty-clay	71.4	28.6	0
						49	10,000	Silty-clay	27.3	72.7	3636
						48	8705	Silty-clay	62.8	37.2	1417
						47	9544	Silty-clay	72.0	28.0	1882
						46	9283	Silty-clay	64.9	35.1	1290
						45	10,000	Silty-clay	100.0	0.0	0
						44	9197	Silty-clay	66.3	33.7	328
						43	10,000	Silt	91.9	8.1	486
						42	10,000	Silt	100.0	0.0	0
						41	10,000	sand	96.9	3.1	0
						40	10,000	sand	100.0	0.0	0
						39	10,000	Sandy silt	70.9	29.1	1060
						38	10,000	Sandy silt	99.2	0.9	0
						37	10,000	Sandy silt	95.9	4.1	0
						36	10,000	Sandy silt	98.4	1.6	0
						35	10,000	Sandy silt	61.6	38.4	1430
						34	10,000	Sandy silt	52.8	47.2	1600
	Early	B	B1-B45	229	N23°41′20″, E69°03′52″ to N23°40′49″, E69°03′48″	33	9298	clay	98.5	1.5	16
						32	10,000	clay	100.0	0.0	0
						31	8456	clay	0.0	89.9	0
						30	10,000	clay	96.0	4.1	0
						29	9614	clay	100.0	0.0	0
						28	10,000	clay	100.0	0.0	0
						27	5181	clay	100.0	0.0	0
						26	10,000	clay	96.8	3.2	0
						25	8939	clay	88.1	11.9	0
						24	9173	Marl	77.7	22.3	0
						23	9925	Marl	86.9	13.1	0
						22	10,000	Marl	77.1	22.9	0
						21	8502	Marl	70.6	29.4	0
						20	10,000	Marl	87.5	9.4	7
						19	9154	Marl	97.1	2.9	0
Bathonian	Late	A	A4-A8	48	N23°41′45.3″, E69°04′13.1″	18	10,000	Marl	93.5	4.0	0
						17	9494	Marl	89.7	10.3	26
						16	10,000	Marl	86.4	13.6	0
						15	10,000	Marl	96.2	3.8	29
						14	8722	Marl	88.8	11.2	0

(continued on next page)

Table 1 (*continued*)

Age	Ammonite bed nos (Fig. 1)	Thickness (m)	GPS location	Foram sample nos. (this study)	total benthic count	Sediment type	% Epifaunal	% Infaunal	Reophax
				13	7578	Marl	96.1	3.9	0
				12	8168	Marl	89.9	10.1	10
				11	9916	Marl	75.6	22.3	0
				10	7500	Marl	89.4	10.6	0
				9	8512	clay	84.3	15.7	6
				8	9522	clay	88.9	11.1	0
				7	9560	clay	71.9	28.1	231
				6	9198	clay	47.3	52.7	994
				5	9966	clay	95.5	4.5	2
				4	9998	clay	84.1	13.6	0
Middle	A1-A4			3	10,000	clay	87.2	12.8	0
				2	7971	Clayey-silt	95.7	4.3	0
				1	7182	Marl	93.1	6.9	0

Age	% BFOI	Lenticulina spp.	Spirillina spp.	Epistomina spp.	Porcellaneaous	Calcareous	Agglutinated	Taxa_S	Shannon_H	Dominance_D
Callovian	37.2	0	0	1732	0	2367	6174	6	1.72	0.19
	26.5	0	0	0	0	0	12,867	10	1.80	0.24
	16.3	0	0	5349	0	5349	4651	3	0.99	0.40
	20.5	0	732	2195	0	3171	5114	6	1.50	0.27
	22.2	0	516	1610	0	2126	6583	12	2.17	0.15
	15.4	0	0	1875	0	1944	7500	13	2.33	0.12
	12.8	448	0	4030	0	5006	3800	8	1.75	0.21
	20.9	0	222	448	0	670	9330	13	2.36	0.11
	12.1	632	0	4445	0	5077	4923	12	2.18	0.14
	97.9	1567	2866	0	0	5297	108	13	2.19	0.14
	25.3	0	0	1343	0	1399	7743	10	1.93	0.18
	8.2	0	0	7500	0	7500	2500	5	1.52	0.24
	5.6	0	0	8479	0	8511	1270	7	1.52	0.27
	39.0	863	572	0	0	1435	8565	8	1.95	0.16
	39.9	6	495	574	0	1100	7988	17	2.35	0.13
	37.3	238	0	0	0	238	9762	8	1.91	0.17
	21.4	0	0	4497	0	4497	5503	6	1.65	0.21
	59.9	2856	276	4011	0	7143	2857	6	1.62	0.22
	36.4	0	0	2727	0	2727	7273	4	1.34	0.27
	35.8	1336	283	3847	0	5790	2915	12	2.20	0.14
	41.4	2213	941	3714	0	7662	1882	9	2.05	0.14
	50.2	2795	502	2581	0	6451	2832	15	2.39	0.11
	100.0	9677	0	0	0	10,000	0	7	1.83	0.17
	86.0	4270	1168	584	0	7555	1642	21	2.62	0.09
	93.5	8709	484	0	0	9514	486	7	1.37	0.34
	86.1	8611	0	1389	0	10,000	0	6	1.76	0.18
	100.0	8224	1061	0	0	10,000	0	10	1.97	0.16
	100.0	10,000	0	0	0	10,000	0	5	1.52	0.23
	54.4	2980	530	3444	0	7482	2518	16	2.51	0.09
	92.9	9203	0	712	0	10,000	0	7	1.77	0.18
	78.8	6665	754	2117	232	9710	58	18	2.43	0.11
	100.0	7622	2222	0	0	10,000	0	7	1.77	0.18
	70.4	6159	0	0	0	6350	3650	9	2.00	0.15
	66.4	5280	0	0	0	5520	4480	9	1.96	0.16
	65.6	4960	0	3184	0	8206	1092	14	2.33	0.11
	67.5	6753	0	3247	0	10,000	0	8	1.89	0.17
	39.8	0	0	0	0	28	7571	7	1.78	0.18
	64.3	5410	750	3435	0	9595	405	12	2.30	0.11

(*continued on next page*)

Table 1 (*continued*)

Age	% BFOI	Lenticulina spp.	Spirillina spp.	Epistomina spp.	Porcellaneaous	Calcareous	Agglutinated	Taxa_S	Shannon_H	Dominance_D
	38.9	3597	0	5873	0	9614	0	10	2.03	0.15
	57.4	5739	0	4261	0	10,000	0	9	1.89	0.18
	66.8	2863	596	1722	0	5181	0	8	1.93	0.16
	95.7	8064	968	0	215	9355	430	11	1.99	0.17
	75.1	5035	610	1539	0	8249	690	15	2.44	0.10
	41.9	2390	971	3475	292	7031	1850	14	2.47	0.10
	82.8	6413	1521	695	0	8948	977	17	2.45	0.10
	66.3	4578	723	2410	0	8554	1446	9	2.06	0.14
	53.3	1006	1997	1498	0	6501	2001	8	1.88	0.16
	80.6	4966	1856	1929	0	9679	321	13	2.21	0.12
	66.7	4200	1640	2715	0	8824	330	13	2.26	0.12
Bathonian	97.5	4246	5105	0	0	9498	502	13	1.84	0.22
	99.7	4551	3943	0	0	9443	51	13	2.06	0.16
	88.1	3547	3995	0	0	8911	1089	24	2.63	0.10
	92.4	4948	3997	0	0	8945	1055	16	2.15	0.16
	90.4	3487	2763	763	0	8528	194	14	2.36	0.11
	97.6	5825	1261	0	0	7393	185	19	2.31	0.12
	81.3	3774	2111	1456	0	8153	15	16	2.32	0.13
	92.0	4994	1875	0	0	9069	847	34	2.97	0.07
	90.5	1357	3645	0	0	6703	797	19	2.17	0.19
	89.4	4289	1582	351	0	8029	483	25	2.68	0.09
	92.4	3054	4741	196	0	9120	402	25	2.41	0.16
	93.3	6578	0	0	0	7098	2462	20	2.42	0.14
	83.5	3855	168	0	0	4023	5175	15	2.43	0.11
	83.0	3663	2740	0	0	8354	1612	26	2.56	0.11
	93.1	6028	1862	0	0	9235	763	26	2.64	0.09
	93.9	5203	3044	0	0	9531	469	24	2.71	0.09
	92.6	4681	2368	353	0	7948	23	15	2.21	0.14
	96.2	3717	2153	249	0	7159	23	21	2.21	0.16

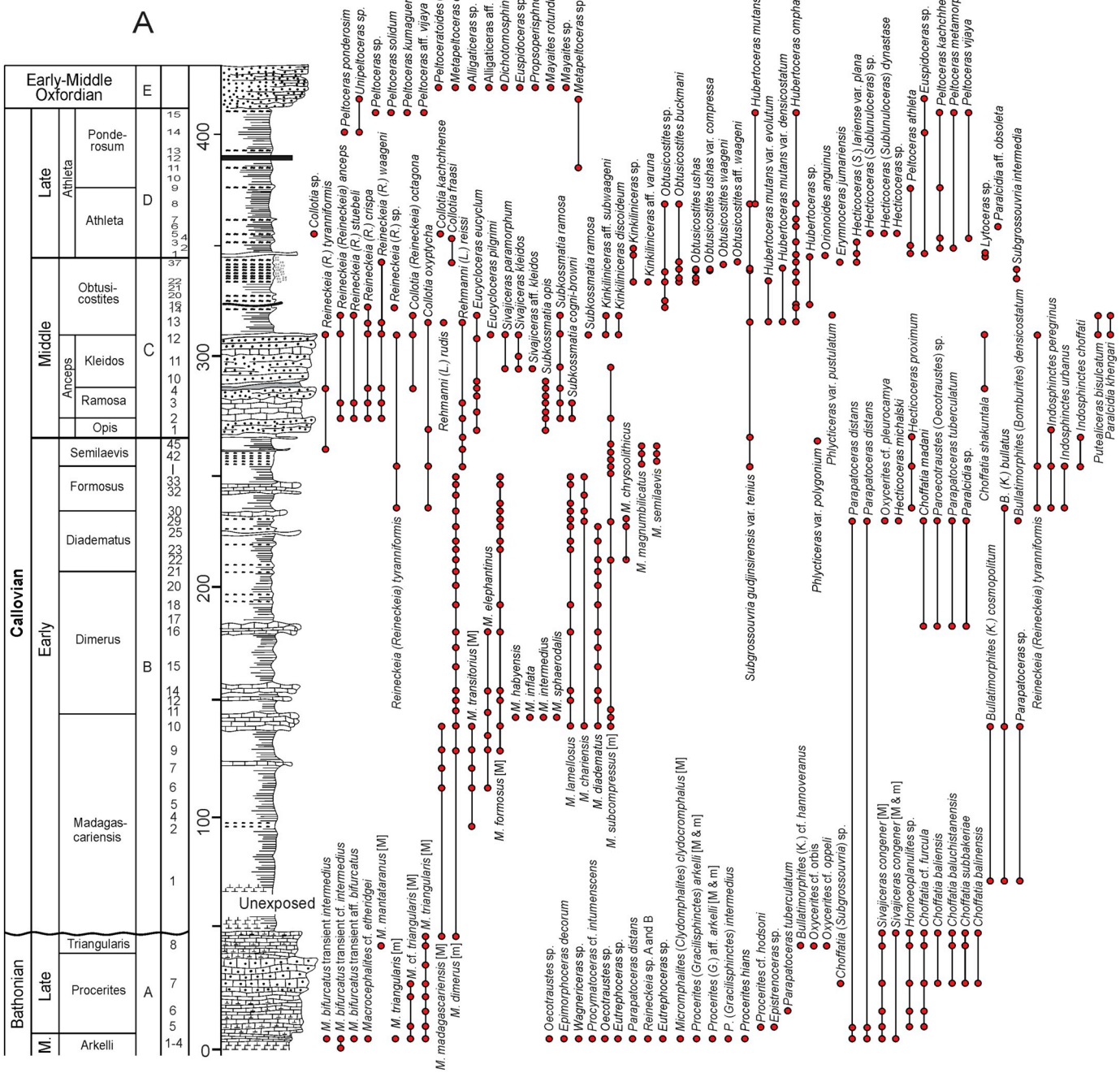

Fig. 2. Biostratigraphy of the Jumara Dome (after Jain, 1996; Jain et al., 1996; Jain, 2014).

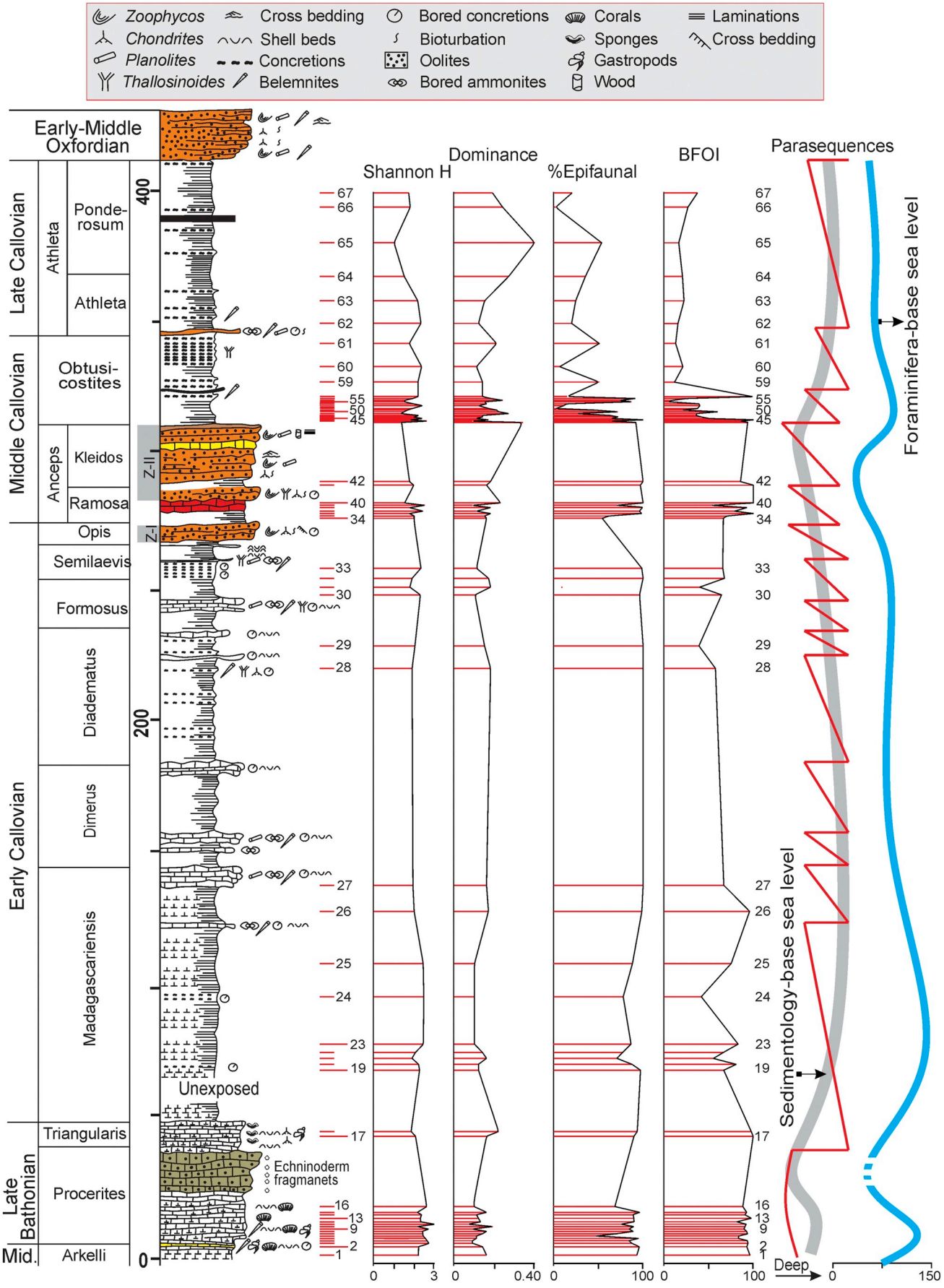

Fig. 3. Stratigraphic log of the Jurassic sedimentary succession exposed at Jumara section showing sample positions (1–67) and biotic traits of the benthic foraminifera with identified parasequences and inferred sea level curves (sedimentology– and benthic foraminifera–based, respectively) from this study.

Table 2
Species identified in the present study with their life-style and oxygenation preference. The life-style is according to test morphology (morphogroups) based on the interpretation of Jurassic (Nagy, 1992; Tyszka, 1994b; Reolid et al., 2008a, 2012; Rita et al., 2016) and modern forms (e.g., Corliss, 1985, 1991; Jones and Charnock, 1985; Bernhard, 1986; Corliss and Chen, 1988; Kaiho, 1991, 1994).

Species	Life-style	Oxy.	Species	Life-style	Oxy.	Species	Life-style	Oxy.
Ammobaculites cobbani	SI	Dysoxic	Astacolus anceps	SI	Oxic	Pyramidlina rara	SI	Suboxic
Ammobaculites coprolithiformis	SI	Dysoxic	Astacolus aphrastus	SI	Oxic	Ramulina abscissa	E	Suboxic
Ammobaculites fontinensis	SI	Dysoxic	Astacolus pauperatus	SI	Oxic	Ramulina apheilolocula	E	Suboxic
Ammobaculites hagni	SI	Dysoxic	Citharina clathrata	SI	Oxic	Tubinella inornata	SI	Suboxic
Ammobaculites reophaciformis	SI	Dysoxic	Citharina colliezi	SI	Oxic			
Ammobaculites subcretaceus	SI	Dysoxic	Citharina flabellata	SI	Oxic			
Ammodiscus aspera	E	Dysoxic	Citharinella compara	SI	Oxic			
Ammodiscus siliceus	E	Dysoxic	Citharinella latifolia	SI	Oxic			
Ammomarginulina cragini	SI	Dysoxic	Citharinella rhomboidea	SI	Oxic			
Dorothia poddari	S to DI	Dysoxic	Dentalina filiformis	SI	Oxic			
Dorothia prekummi	S to DI	Dysoxic	Dentalina guembeli	SI	Oxic			
Eoguttulina polygona	S to DI	Dysoxic	Dentalina subguttifera	SI	Oxic			
Epistomina alveolata	E	Dysoxic	Frondicularia franconica	E	Oxic			
Epistomina cf. ghoshi	E	Dysoxic	Haplophragmium inconstans	SI	Oxic			
Epistomina coronata	E	Dysoxic	Haplophragmium kutchensis	SI	Dysoxic			
Epistomina khawdensis	E	Dysoxic	Haplophragmoides bartensteini	E to SI	Oxic			
Epistomina majungaensis	E	Dysoxic	Haplophragmoides cf. rajnathi	E to SI	Oxic			
Epistomina mosquensis	E	Dysoxic	Haplophragmoides aequale	E to SI	Oxic			
Epistomina preventriosa	E	Dysoxic	Lagena sulcata	E to SI	Suboxic			
Epistomina regularis	E	Dysoxic	Lenticulina bulla	E	Oxic			
Marginulina cf. woodi	SI	Dysoxic	Lenticulina dilectaformis	E	Oxic			
Marginulina cryptospira	SI	Dysoxic	Lenticulina discipiens	E	Oxic			
Marginulina haynesi	SI	Dysoxic	Lenticulina gaultina	E	Oxic			
Marginulina oolithica	SI	Dysoxic	Lenticulina lithuanica	E	Oxic			
Marginulina oxfordiana	SI	Dysoxic	Lenticulina muensteri	E	Oxic			
Marginulina stratifera	SI	Dysoxic	Lenticulina quenstedti	E	Oxic			
Marginulinopsis sp.	SI	Dysoxic	Lenticulina rajnathi	E	Oxic			
Reophax hounstoutensis	S to DI	Dysoxic	Lenticulina subalata	E	Oxic			
Reophax metensis	S to DI	Dysoxic	Lenticulina suturifusus	E	Oxic			
Reophax sterkii	S to DI	Dysoxic	Lenticulina tricarinella	E	Oxic			
Tribrachia inelegans	SI	Dysoxic	Lenticulina varians	E	Oxic			
			Lingulina cf. longiscata	SI	Dysoxic			
			Milimspirella lithuanica	SI	Oxic			
			Nodosaria fontinensis	E to SI	Oxic			
			Nodosaria hortensis	E to SI	Oxic			
			Nodosaria simlex	E to SI	Oxic			
			Nodosaria sowerbyi	E to SI	Oxic			
			Nodosaria sp. 1	E to SI	Oxic			
			Nubeculinella bigoti	E	Oxic			
			Ophthalmidium strumosum	E	Oxic			
			Ophthalmidium carinatum	E	Oxic			
			Palmula deslongchampsi	E to SI	Oxic			
			Patellina subcretacea	E	Oxic			
			Proteonina difflugiformis	SI	Oxic			
			Quinqueloculina Sp.	E	Oxic			
			Reinholdella sp.	E	Oxic			
			Saracenaria oxfordiana	SI	Oxic			
			Saracenaria sp. I	SI	Oxic			
			Saracenaria triquetra	SI	Oxic			
			Spirillina orbicula	E	Oxic			
			Spirillina polygyrata	E	Oxic			
			Spirillina radiata	E	Oxic			
			Textuilaria jurassica	SI	Oxic			
			Triloculina sp.	SI	Oxic			
			Triplasia althoffi	SI	Oxic			
			Triplasia bartensteini	SI	Oxic			
			Tristix oolithica	SI	Oxic			
			Trocholina conosimilis	E	Oxic			
			Vaginulina barnardi	SI	Oxic			
			Vaginulina proxima	SI	Oxic			
			Vaginulina renomina	SI	Oxic			
			Vaginulina sp.	SI	Oxic			
			Vaginulinopsis aduncus	SI	Oxic			
			Vaginulinopsis sp.	SI	Oxic			
			Verneuilinodes subvitreus	SI	Oxic			

For calculating BFOI, the species are grouped as: Oxic (O), Suboxic (S) and Dysoxic (D); see Fig. 3 and text for explanation). Abbreviations: SI = Shallow Infaunal; DI = Deep Infaunal; E – Epifaunal; Oxy. = Oxygenation.

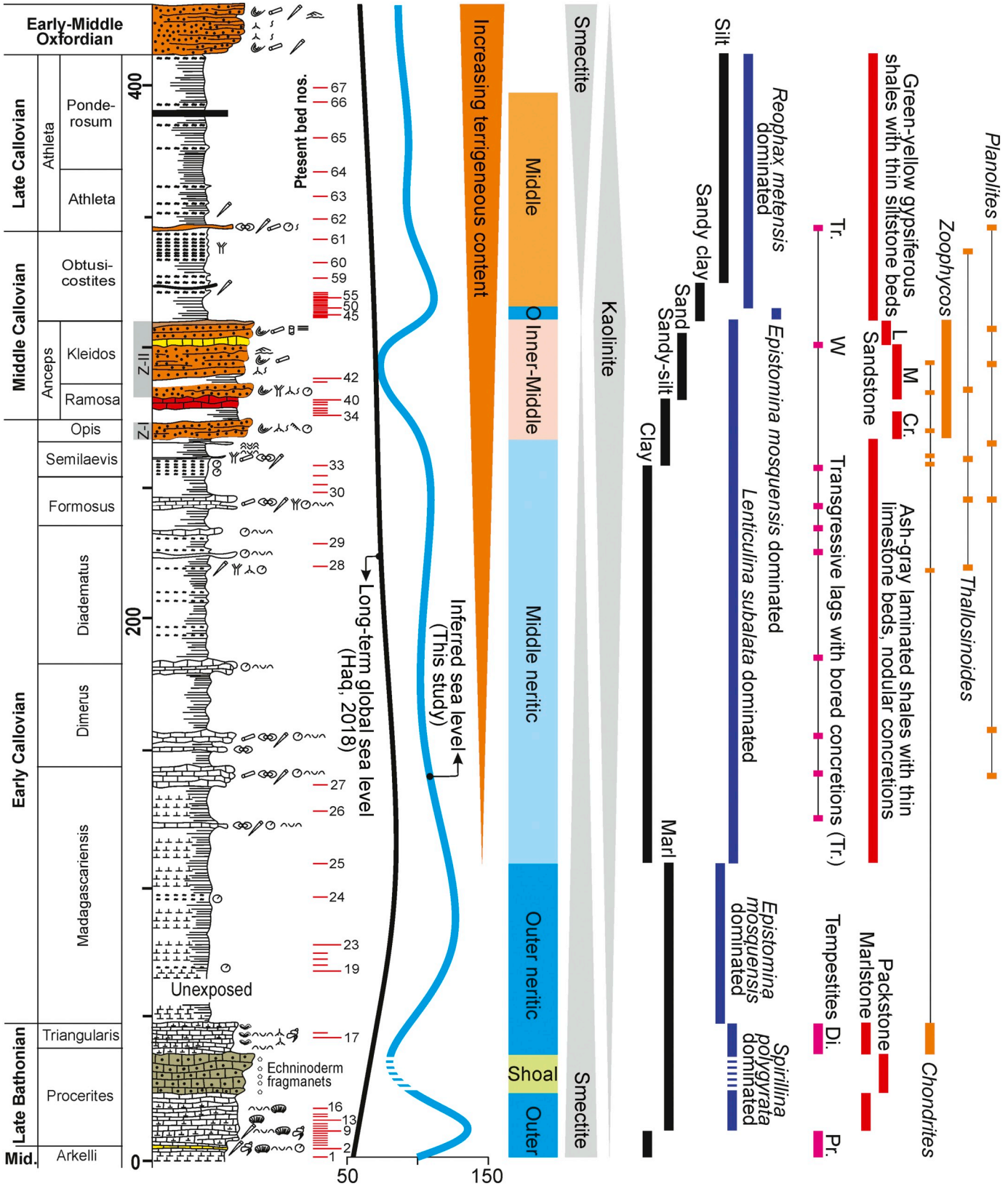

Fig. 4. Inferred relative sea level from present study (solid line) based on biotic and abiotic parameters discussed in the text. The clay composition (Smectite and Kaolinite) trends are after Fürsich et al. (2005). The settling of kaolinite versus smectite is related to basin architecture; due to the relative large size of kaolinite particles, they are generally deposited near the shoreline, whereas smectite, being smaller, is deposited further from the source (see text for further explanation). This trend is quite evident when compared with the inferred relative see level.

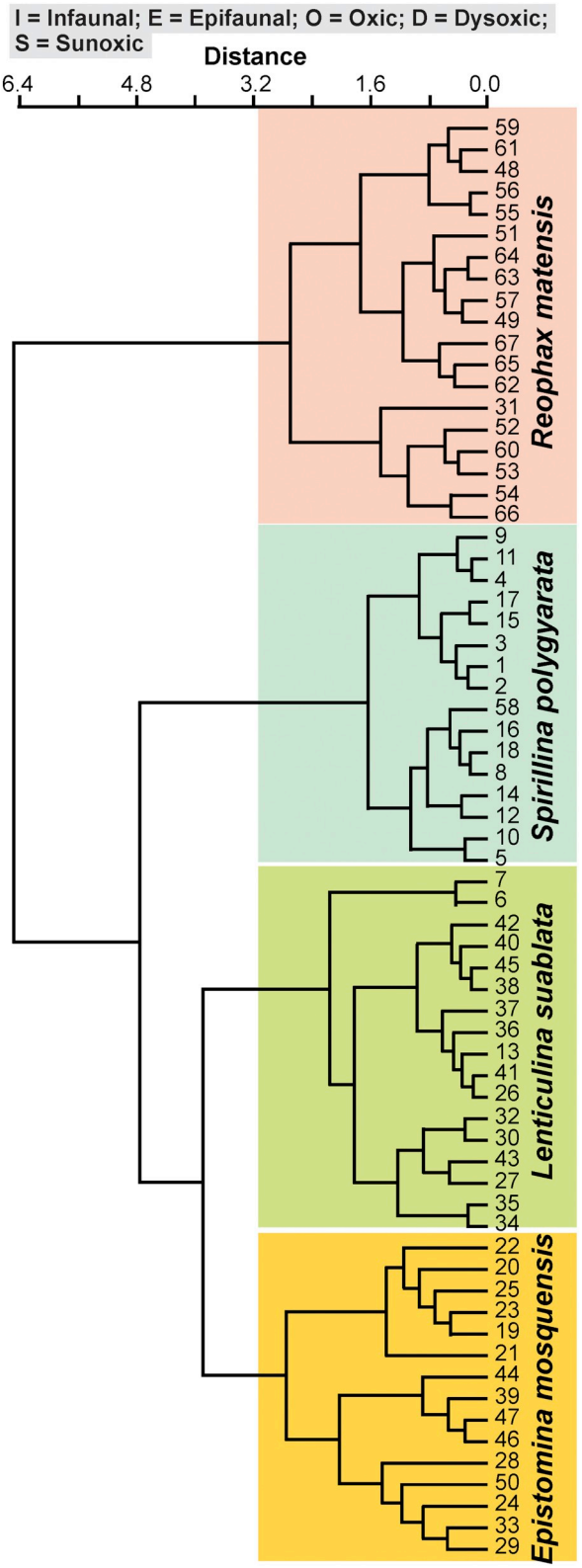

Reophax metensis			%
Reophax metensis	I	D	23.14
Epistomina mosquensis	E	D	18.48
Proteonina difflugiformis	I	O	10.51
Haplophragmoides aequale	I	D	7.97
Epistomina alveolata	E	D	6.07
Haplophragmoides cf. rainathi	I	O	4.62
Textuilaria jurassica	I	O	4.12

Spirillina polygyrata			
Spirillina polygyrata	E	O	25.4
Lenticulina quenstedti	E	O	11.5
Lenticulina bulla	E	O	9.0
Lenticulina subalata	E	O	9.0
Lenticulina dilectaformis	E	O	5.3
Spirillina orbicula	E	O	4.9
Spirillina radiata	E	O	4.0
Lenticulina tricarinella	E	O	3.9
Tubinella inornata	I	S	3.6
Ammodiscus siliceus	E	D	3.0
Ophthalmidium strumosum	E	O	2.6

Lenticulina subalata			
Lenticulina subalata	E	O	21.29
Lenticulina quenstedti	E	O	20.38
Lenticulina dilectaformis	E	O	10.86
Lenticulina bulla	E	O	10.7
Lenticulina muensteri	E	O	7.53
Spirillina polygyrata	E	O	4.81
Epistomina mosquensis	E	D	3.18
Reophax metensis	I	D	2.17

Epistomina mosquensis			
Epistomina mosquensis	E	D	12.5
Lenticulina subalata	E	O	12.3
Spirillina polygyrata	E	O	8.4
Lenticulina muensteri	E	O	7.1
Lenticulina dilectaformis	E	O	6.1
Lenticulina quenstedti	E	O	4.2
Epistomina khawdensis	E	D	4.0
Epistomina alveolata	E	D	4.0
Epistomina regularis	E	D	3.4
Dorothia prekummi	I	D	3.4
Lenticulina tricarinella	E	O	3.3
Reophax metensis	I	D	3.2
Lenticulina bulla	I	O	3.2
Epistomina majungaensis	E	D	3.1
Lenticulina gaultina	E	O	2.9

Fig. 5. Dendrogram of Bray–Curtis–based hierarchical clustering analysis of the benthic foraminifera occurrence data in the Jumara section (Kachchh, India) and faunal composition of the trophic nucleus (taxa represent > 80%) of four potential associations.

axes without or with very little overlap (as noted between *E. mosquensis* and *L. subalata* associations; Fig. 8). Additionally, the percentage of agglutinated taxa (between samples with rare and abundant; Fig. 9A) and between Agglutinated and Calcareous benthic foraminifera also loaded with clear distinction (Figs. 9B). This was also true for Bathonian vs. Callovian (Fig. 9C) and between low and high BFOI samples (Figs. 9D). The Reduced Major axis (RMA) linear regression also gave a significant correlation ($p < .001$) between the NMDS Axis 1 and BFOI value (Fig. 10A; $R^2 = 0.8$) and percentage of agglutinated taxa (Fig. 10B; $R^2 = 0.66$). For the Biotic–abiotic relationships, the

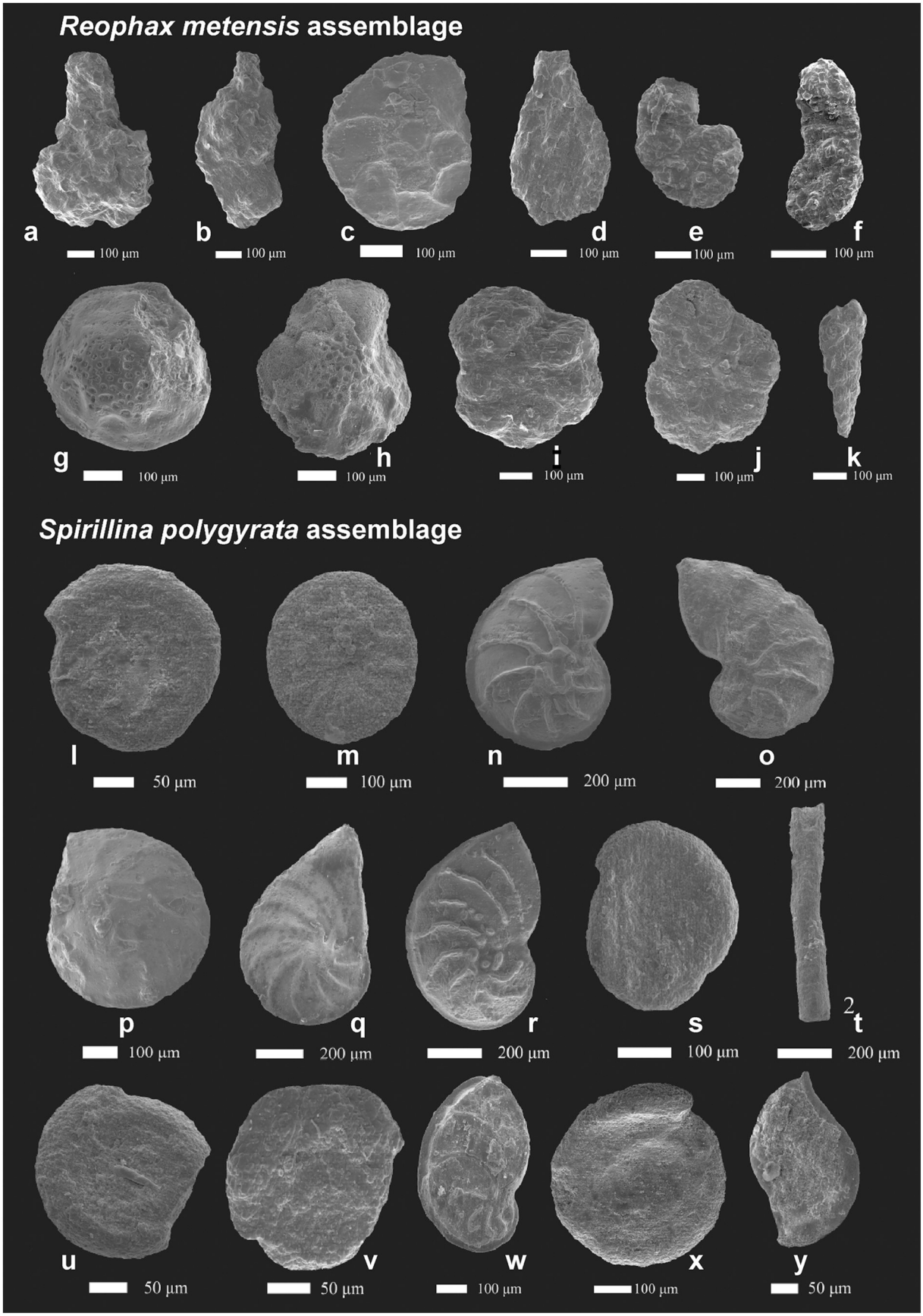

(caption on next page)

Fig. 6. Identified benthic foraminiferal assemblages based on dendrogram (see Fig. 5). *Reophax metensis* Assemblage (a–k): a–b: *Reophax metensis* Franke; Chari–Formation (Callovian), Probe 48; c: *Epistomina mosquensis* Uhlig; Chari–Formation (Callovian), Probe 27; d: *Proteonina difflugiformis* (Brady); Chari–Formation (Callovian), Probe 48; e–f: *Haplophragmium aequale* (Roemer); Chari–Formation (Callovian), Probe 74; g–h: *Epistomina alveolata* Myatliuk; Chari–Formation (Callovian), Probe 74; i–j: *Haplophragmoides* cf. *rajnathi* Bhalla and Abbas; Chari–Formation (Callovian), Probe 35; k: *Textularia jurassica* Gümbel; Chari–Formation (Callovian), Probe 71. *Spirillina polygyrata* Assemblage (l–y): l–m: *Spirillina polygyrata* Guembel; Chari Formation (Callovian), Probe 74; n–o: *Lenticulina quenstedti* (Gümbel); Patcham Formation (Middle Bathonian), Probe 7; p: *Lenticulina bulla* (Lalicker); Patcham Formation (Middle Bathonian), Probe 3; q: *Lenticulina subalata* (Reuss); Chari Formation (Callovian), Probe 93; r: *Lenticulina dilectaformis* Subbotina; Patcham Formation (Middle Bathonian), Probe 2; s: *Spirillina orbicula* Terquem and Berthelin; Patcham Formation (Middle Bathonian), Probe 4; t: *Tubinella inornata* Brady; Patcham Formation (Middle Bathonian), Probe 4; u–v: *Spirillina radiata* Terquem; Chari Formation (Callovian), Probe 43; w: *Lenticulina tricarinella* (Reuss); Patcham Formation (Middle Bathonian), Probe 2; x: *Ammodiscus siliceus* Terquem; Patcham Formation (Middle Bathonian), Probe 3; y: *Ophthalmidium strumosum* (Guembel); Patcham Formation (Middle Bathonian), Probe 4.

RMA linear regressions show significant negative correlations between BFOI and percentage of *Reophax* spp., percentage of infaunal, and sea level (Figs. 11A–C). In addition, BFOI was positively correlated with the percentage of both *Lenticulina* and *Spirillina* (Fig. 11D–E). Moreover, a positive linear correlation was also found between percentage of *Reophax* and sea level (Fig. 11F).

In summary, both Cluster Analysis and NMDS analyses identified sediment type (Fig. 9B), age (Fig. 9C), BFOI, and relative abundance of agglutinated foraminifera (Fig. 10B), sea level and (Fig. 11C and E) as the main factors controlling the distribution of benthic foraminifera in the Jumara section.

4.2. Benthic foraminiferal assemblages

4.2.1. Spirillina polygyrata assemblage (Bathonian)

This assemblage is dominated by *Spirillina polygyrata* (25.4%; Fig. 5) and is characterized by a preference for marls (= pelagic lime mud; limestone–marl intercalations; see Figs. 4–5). Furthermore, it is characterized by high average BFOI value (88.67%), and dominant epifaunal species (80.2%), species diversity (Shannon: 2.35) and low dominance (0.13; Table 3). *Spirillina* is represented by two main species, *S. orbicular* and *S. radiata* (Fig. 5). *Lenticulina quenstedti* is another dominant species (11.5%) and is associated with *L. bulla*, *L. subalata*, *L. delectaformis* and *L. tricarinella* (Fig. 5). Three more species, *Tubinella inorta*, *Ammodiscus siliceous* and *Ophthalmidium strumosum* are of minor occurrence (Fig. 5).

Spirillina is a calcareous epifaunal form that thrives in well–oxygenated environments where sedimentation rates are low (see Gaillard, 1983; Reolid et al., 2008; Springer et al., 2016). In the Jurassic, the abundance of *Spirillina* has been linked to nutrient availability, commonly occurring in mesotrophic settings (Reolid et al., 2008a, 2008b). However, its reduced abundance is also associated with poor availability of oxygen in bottom waters, and thus, independent of food availability (Reolid and Martínez-Ruiz, 2012). Recently, the abundance of *Spirillina* in the mound crest sediments of a former, rich, well–oxygenated, siliceous sponge community has been noted (Bjerager and Surlyk, 2007; Reuter et al., 2013) and attributed to its efficient grazing (Reolid et al., 2008a) and/or epifaunal suspension feeding habit (Langer, 1993). The distribution of *Spirillina* has also been linked to seawater temperature, where its relative abundance peaks are at warmer intervals (during the Bradfordensis Biochron, Aalenian, Middle Jurassic within the Lusitanian Basin, Portugal; Gómez et al., 2009). Interestingly, in Jumara (as in Kachchh), *Spirillina* dominates in the Bathonian carbonates which have been interpreted to represent a semi–arid climate with hot seasonal droughts and higher paleotemperatures of 19–24 °C, as compared to the wet and humid Callovian (Fürsich et al., 2005).

4.2.2. Epistomina mosquensis assemblage (earliest Callovian)

The assemblage is dominated by *Epistomina mosquensis* (12.5%; Fig. 5) and is characterized by a preference for marl–clay substrate. The assemblage is characterized by high average BFOI value (67.1%) and % epifaunal species (78.9), species diversity (Shannon H: 2.22) and low Dominance (0.12) (see Table 3). The assemblage is also dominated by *L. subalata*, *S. polygyrata*, *L. muesteri*, *L. delectaformis*, and *L. quenstedti* (Fig. 5).

Epistomina has been noted to occur in higher abundances in relatively deep waters (outer neritic), in muddy sea bottoms (Le Galvez, 1958; Gradstein, 1978; Bernier, 1984; Stam, 1985; Meyer, 2000; Samson, 2001; Olóriz et al., 2003) or even in shallow waters in fine–grained sediments with low to high mean oxygen levels (Bartenstein and Brand, 1937; Riegraf, 1985; Riegraf and Luterbacher, 1989; Tyszka, 1994a; Sagasti and Ballent, 2002). In the present study, higher diversity and lower Dominance are suggestive of a well-oxygenated bottom waters in an oligotrophic setting. As sediments of this assemblages vary between marl and clay, hence, the oscillation of nutrients and other environmental variables leave no chance for very specific taxa to thrive, where generalized *Epistomina* taxa, flourished. *Epistomina* is a characteristic outer neritic form and similar to the previous *Spirillina* assemblage, also signals deeper outer ramp settings (Fig. 4), as also its brief dominance up section (in samples 44–50), coincident with the total absence of bioturbation in somewhat greenish shales (Fig. 4); both are indicative of deeper offshore and calmer settings.

4.2.3. Lenticulina subalata assemblage (mid– Early to early Middle Callovian)

The assemblage is dominated by *Lenticulina subalata* (21.29%; Fig. 5) and is characterized by a preference for silty substrate. The assemblage is characterized by higher of BFOI value (79.87%) and epifaunal species (87.5%) and by moderate species diversity (Shannon: 1.98) and low dominance (0.16; Table 1). The assemblage is also dominated by species of *Lenticulina* (with *L. subalata*, *L. quenstedti*, *L. delectaformis*, *L. bulla*, and *L. muesteri* with minor abundances of *Spirillina polygyrata*, *Epistomina mosquensis* and *Reophax metensis* (Fig. 5).

Lenticulina, is an opportunistic (r–type strategists), epifaunal to deep infaunal form that occupied a wide range of microhabitats during the Jurassic (Reolid et al., 2008a, 2008b, 2013). Its behavior has been attributed to nutrient input, where an increase in nutrient availability favors its proliferation (Sjoerdsma and Van der Zwaan, 1992; Van der Zwaan et al., 1999). Increasing terrigenous content and decreasing trophic resources favor its increased abundances (see Olóriz et al., 2002; Reolid et al., 2012). *Lenticulina* alone is not a good paleodepth indicator as it has a wide depth range, being recorded from different depths above the CCD (Morris, 1982; Gradstein, 1983; Tyszka, 1994b, 2001), ranging from shallow waters (Morris, 1982; Morris and Coleman, 1989), to middle and outer neritic (Muller Jr, 1990), to inner to outer neritic (Johnson, 1976) and to outer neritic depths (Grunert et al., 2012). Higher abundances of *Lenticulina* in the late Toarcian Lusitanian Basin (Portugal) have been suggested to reflect deepening; *L. muensteri* was noted as a typical species of the distal part of the platform (Henriques and Canales, 2013; Canales Fernández et al., 2014). *Lenticulina* is, however, a very good proxy for well–oxygenated environments (Bernhard, 1986; Koutsoukos et al., 1990; Smolen, 2012).

4.2.4. Reophax metensis assemblage (mid–Middle to Late Callovian)

The assemblage is dominated by *Reophax metensis* (23.1%; Fig. 5) and is characterized by a preference for clay–dominated substrate (see Fig. 4). The *Reophax metensis* assemblage dominates during the Late Callovian. The assemblage is characterized by low values of BFOI (24.9%), % epifaunal species (53.9), and species diversity (Shannon: 1.84) with highest dominance (0.19), and % infaunal species, 46.1% (Fig. 3; Table 3). The assemblage is also dominated by species of *Epistomina mosquensis*, *Proteonina difflugiformis*, *Haplophragmoides aequale*, *Epistomina alveolata*, *Haplophragmoides* cf. *rajnathi* and *Textularia jurassica* (Fig. 5).

Reophax is an opportunistic deep infaunal, detritus and bacterial

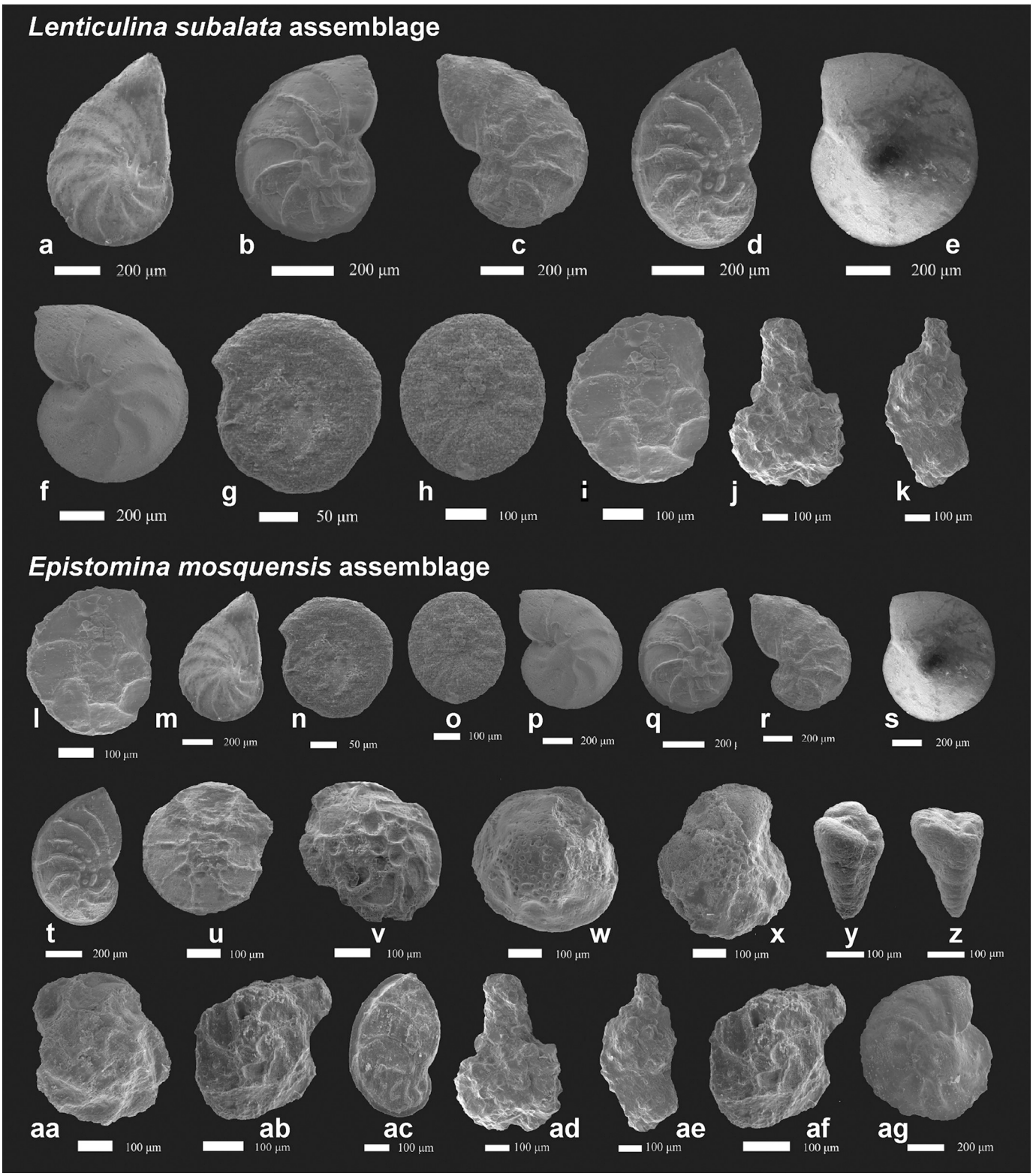

(caption on next page)

Fig. 7. Identified benthic foraminiferal assemblages based on dendrogram (see Fig. 5). *Lenticulina subalata* Assemblage (a–k): a: *Lenticulina subalata* (Reuss); Chari Formation (Callovian), Probe 93; b–c: *Lenticulina quenstedti* (Gümbel); Patcham Formation (Middle Bathonian), Probe 7; d: *Lenticulina dilectaformis* Subbotina; Patcham Formation (Middle Bathonian), Probe 2; e: *Lenticulina bulla* (Lalicker); Patcham Formation (Middle Bathonian), Probe 3; f: *Lenticulina muensteri* (Roemer); Chari Formation (Callovian), Probe 27; g–h: *Spirillina polygyrata* Guembel; Chari Formation (Callovian), Probe 74; i: *Epistomina mosquensis* Uhlig; Chari Formation (Callovian), Probe 27; j–k: *Reophax metensis* Franke; Chari Formation (Callovian), Probe 48. *Epistomina mosquensis* Assemblage (l–ag): l: *Epistomina mosquensis* Uhlig; Chari Formation (Callovian), Probe 27; m: *Lenticulina subalata* (Reuss); Chari Formation (Callovian), Probe 93; n–o: *Spirillina polygyrata* Guembel; Chari Formation (Callovian), Probe 74; p: *Lenticulina muensteri* (Roemer); Chari Formation (Callovian), Probe 27; q–r: *Lenticulina quenstedti* (Gümbel); Patcham Formation (Middle Bathonian), Probe 7; s: *Lenticulina bulla* (Lalicker); Patcham Formation (Middle Bathonian), Probe 3; t: *Lenticulina dilectaformis* Subbotina; Patcham Formation (Middle Bathonian), Probe 2; u–v: *Epistomina khawdensis* (Subbotina, Datta and Srivastava); Chari Formation (Callovian), Probe 27; w–x: *Epistomina alveolata* Myatliuk; Chari–Formation (Callovian), Probe 74; y–z: *Dorothia prekummi* Pandey and Dave; Chari Formation (Callovian), Probe 217, Jhura Dome; aa–ab: *Epistomina regularis* Terquem; Chari Formation (Callovian), Probe 27; ac: *Lenticulina tricarinella* (Reuss); Patcham Formation (Middle Bathonian), Probe 2; ad–ae: *Reophax metensis* Franke; Chari Formation (Callovian), Probe 48; af: *Epistomina majungaensis* Espitalie and Sigal; Chari–Formation (Callovian), Probe 27; ag: *Lenticulina gaultina* (Berthelin); Chari Formation (Callovian), Probe 27.

Table 3
Summary of differences between identified benthic foraminiferal associations (see text for explanation).

	Spirillina polygyrata	*Epistomina mosquensis*	*Lenticulina subalata*	*Reophax metensis*
Age	Bathonian	Earliest Callovian	Early–Middle Callovian	Middle–Late Callovian
Sediment type	Marl	Marl–clay	Clay–dominated	Silt–dominated
BFOI	88.7	67.1	79.9	24.9
% epifaunal	80.2	78.9	87.5	53.9
% infaunal	19.8	21.1	12.5	46.1
% dysoxic	7.8	38.1	13.4	76.3
Shannon H	2.35	2.22	1.98	1.84
Dominance	0.13	0.12	0.16	0.19

eater, whose modern representatives are found burrowing down to 15 cm into the sediment (Kaminski et al., 1988). Under normal marine conditions, the genus is able to live in lowered oxygen levels (−0.5 ml/l) (Kaminski et al., 1995) and have been noted to be the first colonizers (recovery population) after the 1991 Mount Pinatubo eruption (see Hess and Kuhnt, 1996), confirming their opportunistic behavior. Sjoerdsma and Van der Zwaan (1992) noted that the opportunistic behavior of some foraminifera (like *Lenticulina* and *Reophax*) is related to nutrient input, whereby increase in nutrient availability favors proliferation of r–type strategists (see also Reolid and Martínez-Ruiz, 2012).

5. Discussion

Cluster and NMDS analyses identified sediment type (Fig. 9B), age (Fig. 9C), BFOI (Fig. 10A), and sea level (Fig. 11E) as primary factors controlling the distribution of benthic foraminifera. It must be mentioned that BFOI is a function of the availability of oxygen, which in turn, is dependent on availability of nutrients in bottom waters (Kaiho, 1991, 1994; Sjoerdsma and Van der Zwaan, 1992; Van der Zwaan et al., 1999; see discussion below).

The Bathonian is marked by low $\delta^{13}C$ values (0.44 to 0.48‰; average 0.45‰), whereas the Callovian has widely fluctuating values ranging from −0.05 to 1.82‰ (average values: Early: 0.51‰; Middle: 0.32‰ and Late Callovian: 0.96‰; see Fürsich et al., 2005). Assuming a minor role of basinal tectonics, as is the case during the Bathonian–Callovian of the Kachchh Basin (Biswas, 1991; Fürsich et al., 2013), lithology (sediment type) and sea level are closely tied. This is more so, as Kachchh represents a shallow epeiric basin, so the effects of sea level on both lithology and fauna would be pronounced (see also Hallam, 1991).

The strongly bioturbated carbonates of the Bathonian are characterized by rhythmic alternations of bioclastic–rich marls and

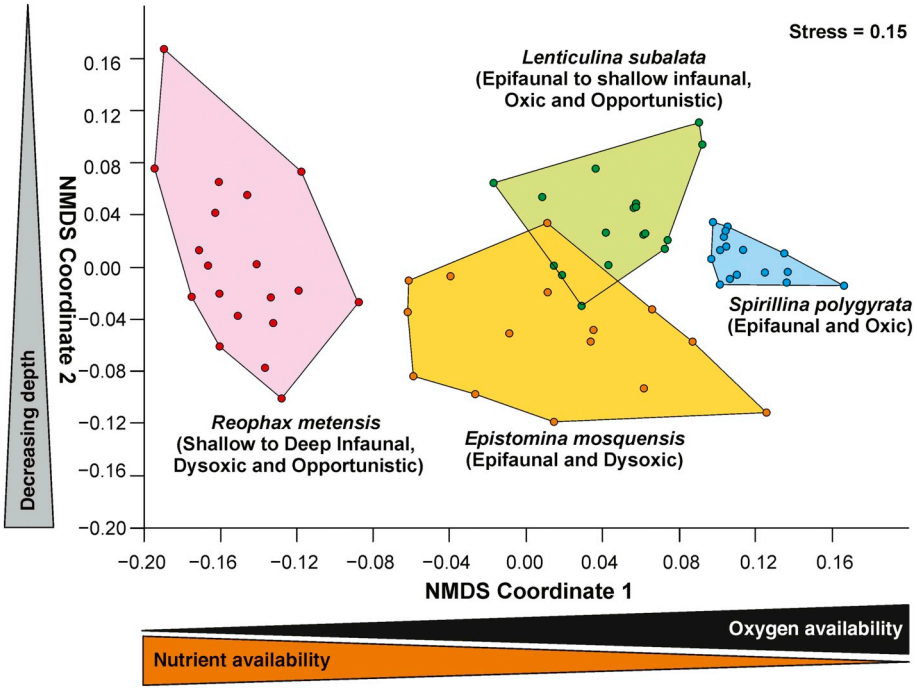

Fig. 8. Nonmetric multidimensional scaling (NMDS) of the concurrence data of show no or little overlap among the cluster–based association (Fig. 5).

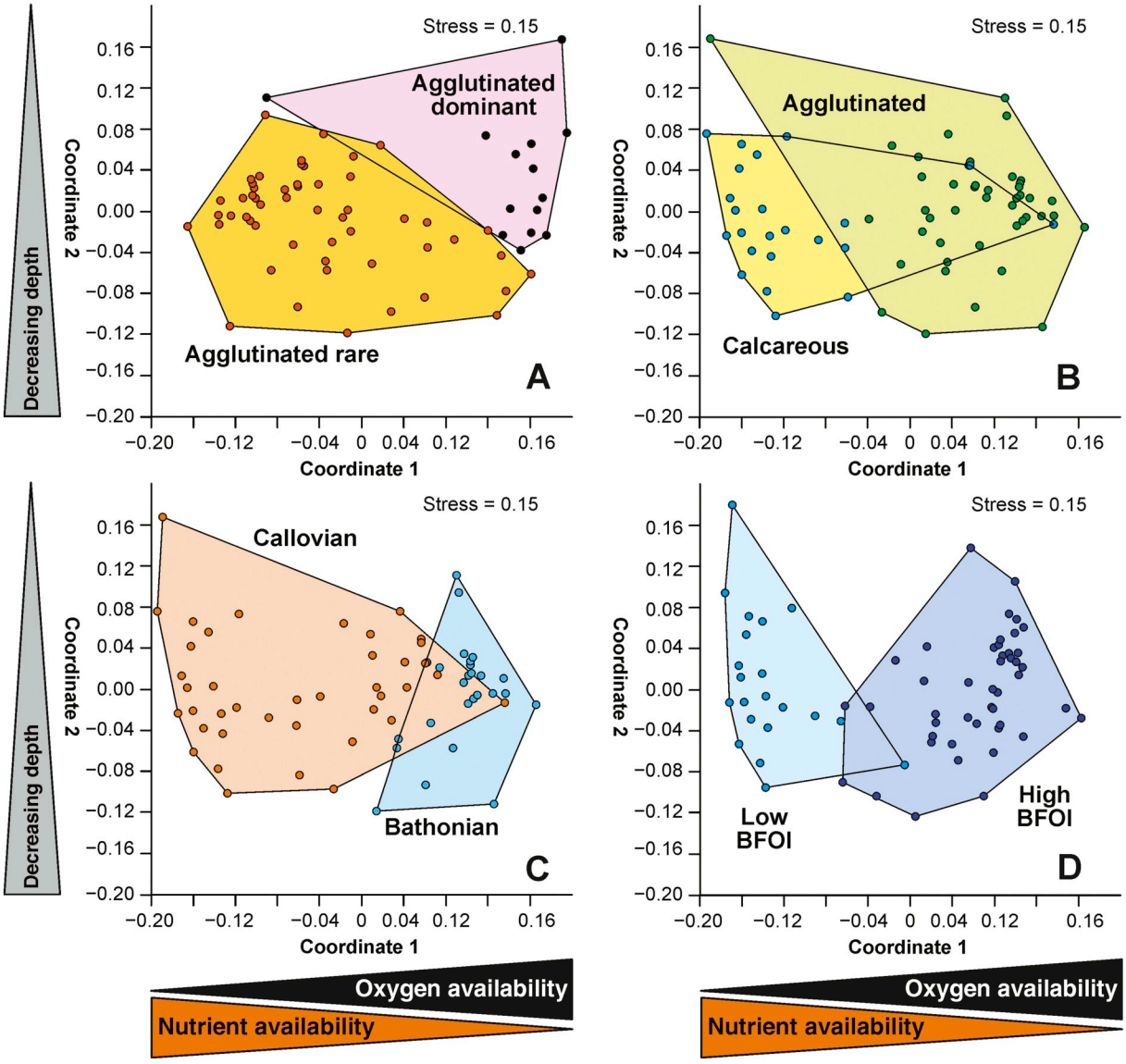

Fig. 9. Nonmetric multidimensional scaling (NMDS) of the concurrence data. A, sample scores coded by agglutinated percentage. B, sample scores coded by dominated shell composition. C, sample scores and siliciclastic depositional systems. C, sample scores coded by Age. D, sample scores coded by BFOI index value.

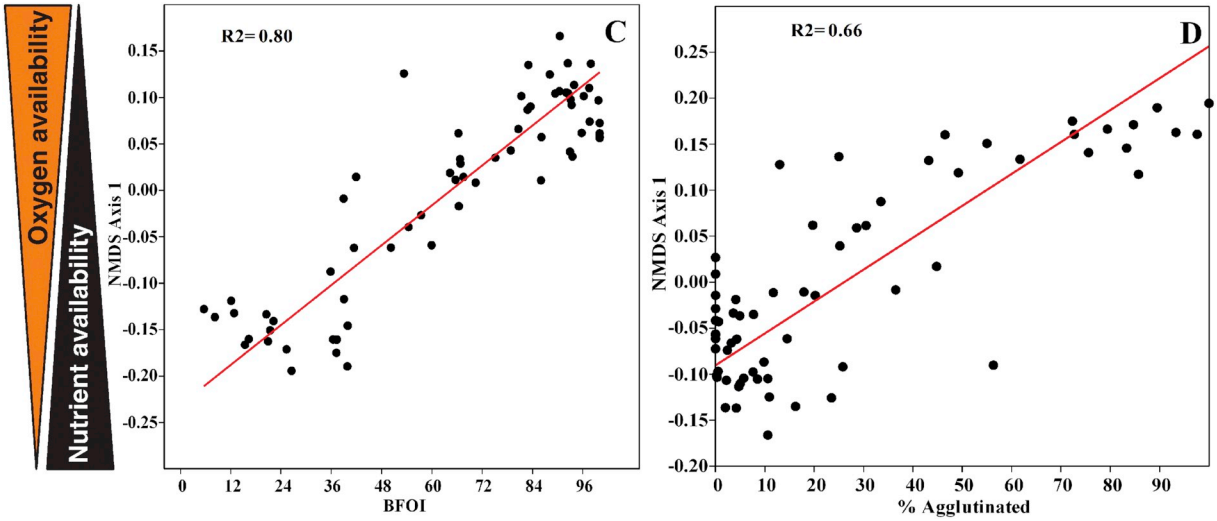

Fig. 10. Reduced Major axis (RMA) linear regression plot between the coordinate 1 of the NMDS and BFOI index (A), between NMDS axis 1 and agglutinated percentage (B).

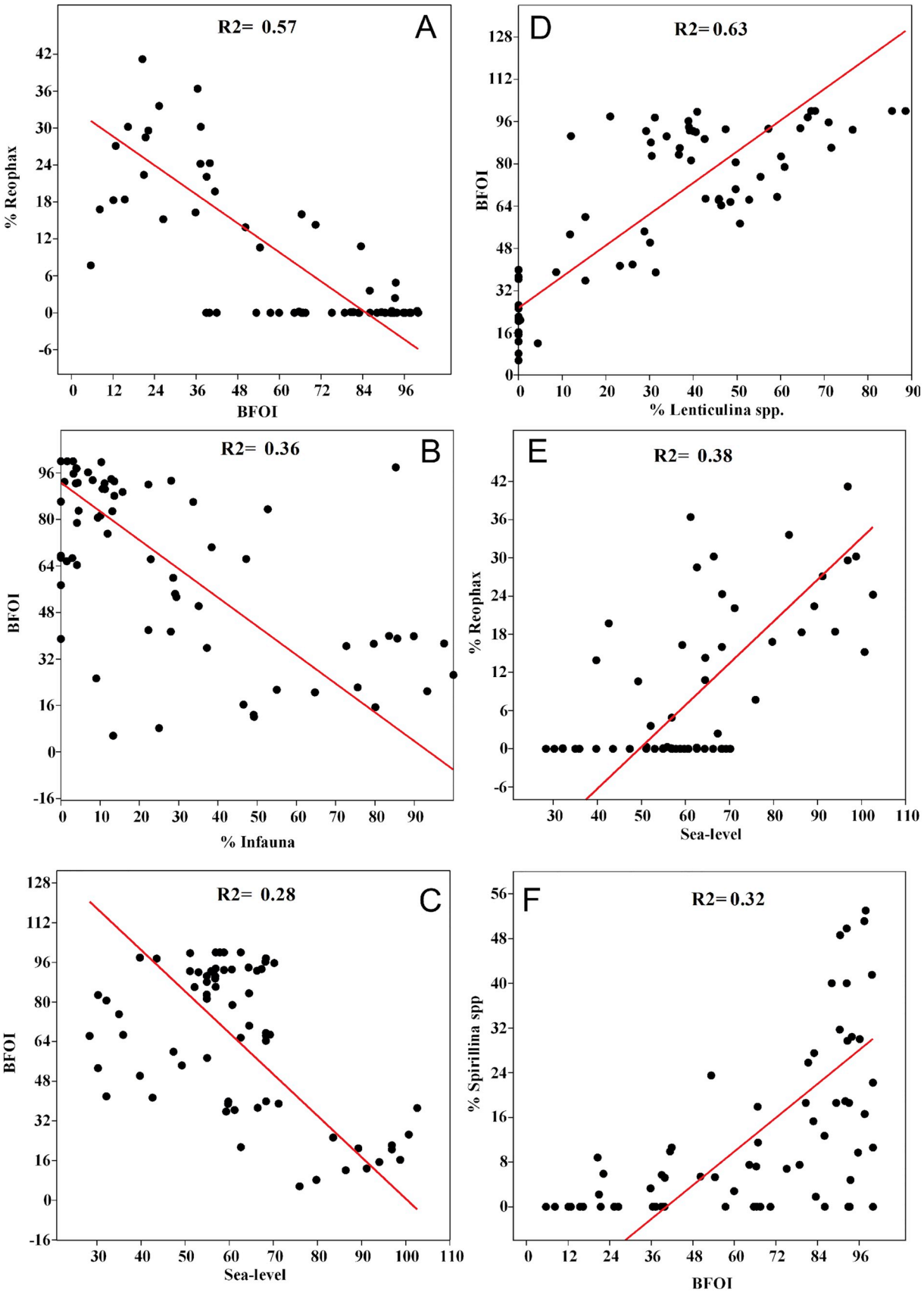

Fig. 11. Biotic–abiotic relationships. A: Reduced Major axis (RMA) linear regression plot between BFOI and % *Reophax* spp., B: BFOI and % Infaunal, C: between sea–level and BFOI, D: between % *Lenticulina* spp., and BFOI, E: sea–level and % *Reophax* spp., and F: between BFOI and % *Spirillina* species.

fine–grained limestones with rare thin shell–rich beds. The limestones are well bedded and range from marlstones, to carbonate mudstones to wackestones. The lithology is typical of an outer neritic setting being deposited in a calm environment that was rarely punctuated by storms resulting in the deposition of thin shell–rich beds (= distal tempestites; see Fig. 4). The presence of abundant corals (at the base) and of sponges (at the top) (Fig. 4), suggest well–oxygenated, clear and warm bottom waters (corals) and within the lower part of the photic zone (sponges) in an outer neritic depth (Fig. 4). These lithological and deeper conditions (also corroborated by the increased abundance of smectite; being more in offshore settings; see Dera et al., 2009) favored the proliferation and dominance of *Spirillina* (see Fig. 4). *Spirillina* prefers middle neritic depths (Murray, 1991: < 100 m). Additionally, the reduced relative abundance of infaunal forms within the *Spirillina* assemblage (Fig. 5 and Table 3) attest to an oligotrophic environment, well corroborated by low $\delta^{13}C$ values (0.45‰; Fürsich et al., 2005). Also, the lack of tubular forms and the dominance of dish–shaped sponges within the upper part of the carbonate section (Figs. 3–4), have been attributed to low nutrient availability and lower rates of sedimentation (see also Krautter, 1997, 1998). Based on a large analysis of bivalve associations, Fürsich et al. (2004) also opined for an environment with nutrient–poor waters for the Bathonian carbonates. The high values of BFOI, epifauna and diversity with reduced species dominance (Fig. 2), also suggest that these deeper conditions harbored a healthy equitable ecosystem. In general, globally also, the Bathonian was also an interval of warmth and rising sea level (Haq, 2018) (see also Fig. 4). Bathonian warming, as in the Kachchh Basin (Fig. 4), is also well-documented for other basinal studies. In Poland, the Late Bajocian–earliest Late Bathonian interval is marked by higher paleotemperatures (18–27 °C), followed by cooling in the latest Bathonian and Callovian (15–22 °C) (Malchus and Steuber, 2002). Additionally, data from France also suggest a similar warm subtropical surface temperatures of 20–27 °C for the entire Bathonian (Dromart et al., 2003).

The transition from Bathonian to earliest Callovian is somewhat gradual in terms of lithology (Fig. 4). The earliest Callovian is marked by the scarce presence of macrofauna (ammonites and bivalves; Figs. 4–5), non–bioturbated sediments, and darker ash–gray marls, suggesting slightly deeper outer neritic depths, in a calm and moderately oxygenated environment. The latter is also corroborated by somewhat reduced values of BFOI, epifauna and species diversity, in comparison to higher Bathonian values (see also Tables 1 and 3). This deeper setting favored the proliferation of another characteristic outer neritic taxa, *Epistomina mosquensis*, and the subsequent abundance decline of *Spirillina* (*S. polygyrata*; Fig. 4; see also Tables 1 and 3). This faunal change mirrors a much larger climatic change within the basin, from a hot and dry Bathonian to a wet and humid Callovian with cooler bottom waters (Fürsich et al., 2005). This change is also reflected in the distinct separation of Bathonian and Callovian samples in the NDMS plot (Fig. 9C). Additionally, *Spirillina* prefers warmer bottom waters, hence, a change in bottom water paleotemperature accentuated its decline in the earliest Callovian, whereas, deeper outer–neritic settings with somewhat reduced oxygen levels, favored the dominance of *Epistomina* (see also Bartenstein and Brand, 1937; Sagasti and Ballent, 2002) (see also Fig. 5). In general, globally also, the Bathonian–Callovian transition is marked by rising sea level up until the European ammonite Bullatus Zone (=Madgascariensis Zone; Fig. 4) and thereafter falling sea levels for the entire Callovian (Haq, 2018) and is corroborated in the present study, also (Fig. 4).

The mid– to late Early Callovian interval is marked by clays - gray, laminated, gypsiferous to micaceous shales with alternating thin bands of shell–rich limestones and siltstones, that in the upper part, have occasional bored concretions and shales that are darker and carbonaceous. This unit is also characterized by multiple coarsening upward sequences (parasequences) whose tops are marked by transgressive lags, suggesting cyclical deposition in an unstable and relatively shallow setting (Figs. 3–4). This shift in lithology from marl to clay, also heralds an increased terrigenous input (= nutrient availability), which is well–reflected in the increasing kaolinite content (corroborating near shore influence; Fig. 4). This clay unit encompasses the *Lenticulina subalata* assemblage (Figs. 4–5). The occurrence of this opportunist, *Lenticulina*, is related to nutrient input, where increased nutrient availability favors its proliferation (Sjoerdsma and Van der Zwaan, 1992; Van der Zwaan et al., 1999). Thus, it is plausible that the fluctuating basinal conditions coupled with increased terrigenous input (= mesotrophic conditions) in somewhat shallower middle neritic settings were ideal conditions for an opportunist like *Lenticulina*, to proliferate (Fig. 4).

During the succeeding early to mid–Middle Callovian interval, the opportunist behavior of *Lenticulina* is well illustrated as it dominates even when there is a regime change, in terms of increased rate of sedimentation, higher energy (cross bedding), shallower setting (= maximum abundance of kaolinite content) and the deposition of medium–grained sandy–silt to sand (Zoophycos Sandstone I; Jain, 1996; see Fig. 4). Both *L. subalata* and *L. quenstedti* dominate this interval (Fig. 5); in some samples as much as 80 to 100% (samples 38–42; see Fig. 3), well reflected in the high species dominance and reduced diversity for this brief interval (see Fig. 3). Both the opportunist and the epifaunal mode of life (as also noted for its extant occurrences), is quite evident in this study; *Lenticulina* thrives not only in calm, warm, clear and oligotrophic settings in the Bathonian at deeper paleodepths but also in shallower, muddy and mesotrophic settings of higher energy in the Callovian (Fig. 4).

Additionally, the *Lenticulina* assemblage (samples 26–45; Figs. 3–4) is marked by two major lithological units, lower clays and upper sands (and silty sands; Fig. 4). The clays are ash–gray with bored concretions, and marked by multiple coarsening upward cycles (parasequences), starting with finer clays and ending in somewhat coarser thin–bedded shell (mostly horizontally oriented) bearing limestone with sharp erosive bases. All there are indicative of deposition below the Fair Weather Wave Base but occasionally interrupted by storms that resulted in the deposition of lag deposits (transgressive lags) in shallower middle neritic depths, where terrigenous input from the shore was constantly increasing through time (higher kaolinite content; Dera et al., 2009; Hesselbo et al., 2009; see Fig. 3). Up section (samples 39–45; Fig. 4) coarser sands (cross–bedded, massive and then laminated sandstones) and increased kaolinite (near shore indicator), suggests a somewhat inner to middle neritic depth, rather than outer neritic. This shallower paleodepth for *Lenticulina* exemplifies its opportunistic nature where it is able to adapt to higher nutrients and shallower depths (Fig. 4). Additionally, a strong and significant correlation of *Lenticulina* with BFOI ($R^2 = 0.63$; Fig. 11C), reaffirms its oft demonstrated preference for well–oxygenated environments (see also Bernhard, 1986; Koutsoukos et al., 1990; Smolen, 2012).

A sudden regime change is noted since the mid– Middle Callovian (from the base of Obtusicostites Zone; Fig. 2–4), from sand to sandy clay and silt, marked by greenish–yellow gypsiferous shales with thin–-bedded siltstones, interspersed with ferruginous and calcareous nodules (Fig. 4). Throughout this gypsiferous unit (gypsum is most likely the oxidation product of pyrite reacting with Ca^{2+} ions; secondary gypsum), from the base to top, there is a gradual increase in sand content (terrigenous input) and smectite, with occasional levels containing the opportunistic *Bositra*–dominated low–diversity bivalve faunas (see also Fürsich et al., 1991). In the present study, the opportunistic deep infaunal taxa *Reophax metensis* dominates this unit and forms a distinct assemblage (Figs. 4–5). Sjoerdsma and Van der Zwaan (1992) noted that the opportunistic behavior of some foraminifera (like *Lenticulina* and *Reophax*) is related to nutrient input, whereby nutrient increase favors proliferation of such r–type strategists (see also Reolid

and Martínez-Ruiz, 2012). The dominance of infaunal species in this assemblage (Fig. 5; see Table 3) also corroborates this inference. Additionally, this assemblage is also marked by lower species diversity, epifauna, and BFOI values with very high species dominance suggesting a somewhat stressed environment (Fig. 3). Both *Reophax and Epistomina* prefer middle neritic depth (Fig. 4). In general, globally also, the Middle to late Callovian interval is marked by declining sea levels (Haq, 2018), Kachchh being a shallow basin, its effects on fauna and substrate are accordingly somewhat more accentuated (see Fig. 4).

Interestingly, the relationship between BFOI and *Reophax* is negative and statically significant ($R^2 = 0.58$), suggesting that its distribution is influenced by oxygen availability, and to a lesser extent by sea level (positive and significant; $R^2 = 0.38$; Fig. 8E). Its preference for lowered oxygen conditions (*meso-* to eutrophic conditions) is well-documented (see Kaminski et al., 1988; Kaminski et al., 1995). Contextually, it is interesting to note that BFOI is also significantly and negatively correlated with infaunal percentage ($R^2 = 0.36$; Fig. 8B). This inverse relationship would be expected, as the oxidation of increased nutrients would take up the available oxygen, rendering the environment somewhat dysoxic (oxygen–deficient) and thus, favoring the dominance of *Reophax metensis*, as noted here (Fig. 5). Additionally, lower BFOI value and higher species dominance point to environmental stress. The dominance of silt and increased input of smectite and reduced kaolinite content are indicative of somewhat shallower middle neritic setting (see Hallam et al., 1991; Dera et al., 2009; Hesselbo et al., 2009) (Fig. 4), well corroborated by the presence of shallow water agglutinated taxa, *Proteonina difflugiformis*, *Haplophragmoides aequale*, *H.* cf. *rajnathi* and *Textularia jurassica* (Fig. 5).

The forgoing discussion demonstrates the overriding role of both sediment type and sea level in shaping the benthic foraminiferal distribution pattern. The NMDS pattern shows that the taxa with different shell composition (agglutinated vs calcareous) have different environmental preferences. BFOI strongly correlates with the NDMS Axis 1 ($R^2 = 0.80$; Fig. 10A) suggesting that the availability of oxygen is a significant factor affecting the distribution of benthic foraminifera. In fact, samples with low (< 50%) and high BFOI values (> 50%) plot significantly separate in the NDMS plot, also (Fig. 9D), reaffirming the strong influence of oxygen availability in bottom waters in shaping the distribution of benthic foraminifera. In simple terms, the availability of oxygen is a function of nutrient availability, the more the latter, the less the former (TROX model of Jorissen et al., 1995; see also Sjoerdsma and Van der Zwaan, 1992; Jain et al., 2007). The negative and statistically significant ($R^2 = 0.28$; Fig. 11C) relationship between BFOI and sea level, could be a reflection of limited water circulation when depth increases to a certain level (Abdelhady et al., 2019). In addition, low energy settings, below wave/storm base, enhance pelagic sedimentation that is rich in organic matter, where its decay consumes available oxygen, thereby resulting in hypoxia (Abdelhady and Fürsich, 2014). In modern settings, transgressive episodes are, at times, associated with decreasing oxygen availability resulting in the shoreward migration of the oxygen minimum zone (OMZ) (Bond and Wignall, 2008; Gambacorta et al., 2016). This decline in dissolved oxygen availability, is further exacerbated by the increased delivery of nutrients to the marine shelf by terrestrial runoff, and additionally, when coupled with water column stratification due to salinity contrasts and high surface sea water temperatures, leads to deficiency of oxygen at the sea floor and a subsequent increase in infaunal and/or opportunistic forms that thrive in such dysoxic conditions (Bond and Wignall, 2008). Increasing terrigenous influx along with wet and humid conditions in the Callovian for the Kachchh Basin (Fürsich et al., 2005), could have provided the necessary trigger for the observed assemblages changes. This is also corroborated by the disappearance of bioturbators (= the absence of bioturbated sediments, in the present case), that are considered fair indictors of water column anoxia or declining dissolved oxygen availability (dysoxia). However, such a scenario can only be confirmed by high–resolution geochemical analyses (of redox conditions).

6. Conclusions

The changes in the distribution pattern of benthic foraminifera coupled with sedimentological and mineralogical data and quantitative analyses (Clustering and NMDS ordination) has enabled a plausible reconstruction for the paleoenvironment of the studied Jumara section (Kachchh Basin, India). This analyses has yielded four distinct and statistically significant benthic foraminiferal associations along with their abiotic and biotic traits, occupying different environmental settings spanning specific times. Diversity and epifaunal/infaunal ratio reflect a cyclic pattern comparable to those of third order sea–level fluctuations.

The Bathonian represents an outer neritic depth with higher carbonate production in a healthy ecosystem dominated by carbonate shells with limited terrigenous influx (oligotrophic regime) in an arid climate, where equitable biotopes were developed (= *Spirillina polygyrata* and *Epistomina mosquensis* assemblages). In contrast, the Callovian represents a gradual shift towards a more humid climate and increased terrigenous input in a relatively shallower setting with meso–eutrophic regimes with periodic hypoxia, resulting in less diverse and high dominance assemblages (= *Lenticulina subalata* and *Reophax metensis* assemblages).

Acknowledgements

The authors are grateful to two anonymous reviewers for constructive comments and suggestions that greatly improved the manuscript. SJ gratefully acknowledges literature help from Dr. Michael Kaminski (Saudi Arabia) and Dmitry Ruban (Russia).

References

Abdelhady, A.A., Fürsich, F.T., 2014. Macroinvertebrate palaeo–communities from the Jurassic succession of Gebel Maghara (Sinai, Egypt). J. Afr. Earth Sci. 97, 173–193.
Abdelhady, A.A., Fürsich, F.T., 2015. Palaeobiogeography of the Bajocian–Oxfordian macrofauna of Gebel Maghara (North Sinai, Egypt): implications for eustacy and basin topography. Palaeogeogr. Palaeoclimatol. Palaeoecol. 417, 261–273.
Abdelhady, A.A., Mohamed, R.S.A., 2017. Paucispecific macroinvertebrate communities in the Upper cretaceous of El Hassana Dome (Abu Roash, Egypt): Environmental controls vs adaptive strategies. Cretac. Res. 74, 120–136.
Abdelhady, A.A., Mahmoud, M.K., Ismail, E., Fan, J., Zhang, S., Xiao, J., 2019. Water chemistry and substrate type as major determinants of molluscan feeding habit and life–mode in lagoon sediments. Estuar. Coast. Shelf Sci. 220, 120–130.
Alhussein, M., 2010. Taxonomie und palökologie der benthischen Foraminiferen aus dem Mitteljura des Kachchh–Beckens, westliches Indien. (Unpublished Thesis, 160 pp.).
Alhussein, M., 2014. Taxonomy of the Middle Jurassic benthic foraminifera of the Kachchh Basin, Western India. Beringeria 44, 51–105.
Bartenstein, H., Brand, E., 1937. Mikro–paläontologische untersuchungen zur stratigraphie des nordwest–deutschen Lias und Doggers. Abh. Senckenb. Naturforsch. Ges. 439, 1–224.
Bernhard, J.M., 1986. Characteristic assemblages and morphologies from anoxic organic rich deposits: Jurassic through Holocene. J. Foraminifer. Res. 16, 207–215.
Bernier, P., 1984. Les formations carbonatées du Kimméridgien et du Portlandien dans le Jura méridional. Stratigraphie, micropaléontologie, sédimentologie. (Doc. Lab. Géol. Lyon 92, 803 pp.).
Bhalla, S.N., Abbas, S.M., 1978. Jurassic foraminifera from Kutch, India. Micropaleontology 24, 160–209.
Bhalla, S.N., Talib, A., 1991. Callovian–Oxfordian foraminifera from Jhurio hill, Kutch, Western India. Rev. Paláeobiol. 10, 85–114.
Biswas, S.K., 1991. Stratigraphy and sedimentary evolution of the Mesozoic basin of Kutch, western India. In: Tandon, S.K., Pant, C.C., Casshyap, S.M. (Eds.), Stratigraphy and Sedimentary Evolution of Western India. Gyanodaya Prakashan, Nainital, pp. 74–103.
Bjerager, M., Surlyk, F., 2007. Benthic palaeoecology of Danian deep–shelf bryozoan mounds in the Danish Basin. Palaeogeogr. Palaeoclimatol. Palaeoecol. 250 (1–4), 184–215.
Bond, D.P.G., Wignall, P.B., 2008. The role of sea–level change and marine anoxia in the Frasnian–Famennian (late Devonian) mass extinction. Palaeogeogr. Palaeoclimatol. Palaeoecol. 263, 107–118.
Canales Fernández, M.L., García–Baquero, G., Henriques, M.H., Figueiredo, V.L., 2014. Palaeoecological distribution pattern of Early–Middle Jurassic benthic foraminifera in the Lusitanian Basin (Portugal) based on multivariate analysis. Palaeogeogr. Palaeoclimatol. Palaeoecol. 410, 14–26.
Corliss, B.H., 1985. Microhabitats of benthic foraminifera within deep-sea sediments. Nature 314, 435–438.
Corliss, B.H., 1991. Morphology and microhabitat preferences of benthic foraminifera

from the Northwest Atlantic Ocean. Mar. Micropaleontol. 17, 195–236.
Corliss, B.H., Chen, C., 1988. Morphotype patterns of Norwegian deep sea benthic foraminifera and ecological implications. Geology 16, 716–719.
Dera, G., Pellenard, P., Neige, P., Deconinck, J., Pucéat, E., Dommergues, J., 2009. Distribution of clay minerals in early Jurassic Peritethyan seas: palaeoclimatic significance inferred from multiproxy comparisons. Palaeogeogr. Palaeoclimatol. Palaeoecol. 271, 39–51.
Dromart, G., Garcia, J.-P., Gaumet, F., Picard, S., Rousseau, M., Atrops, F., Lécuyer, C., Sheppard, S.M.F., 2003. Perturbation of the carbon cycle at the Middle/late Jurassic transition: geological and geochemical evidence. Am. J. Sci. 303, 667–707.
Fürsich, F.T., Oschmann, W., 1993. Shell beds as tools in Basin analysis, the Jurassic of Kachchh, western India. J. Geol. Soc. Lond. 150, 169–185.
Fürsich, F.T., Pandey, D.K., 2003. Sequence stratigraphic significance of sedimentary cycles and shell concentrations in the Upper Jurassic–Lower Cretaceous of Kachchh, western India. Palaeogeogr. Palaeoclimatol. Palaeoecol. 193 (2), 285–309.
Fürsich, F.T., Werner, W., 1986. Benthic associations and their environmental significance in the Lusitanian Basin (Upper Jurassic, Portugal). Neues Jb. Geol. Paläontol. Abh. 172, 271–329.
Fürsich, F.T., Oschmann, W., Jaitly, A.K., Singh, I.B., 1991. Faunal response to transgressive–regressive cycles: example from the Jurassic of western India. Palaeogeogr. Palaeoclimatol. Palaeoecol. 85, 149–159.
Fürsich, F.T., Oschmann, W., Singh, I.B., Jaitly, A.K., 1992. Hardgrounds, reworked concretion levels and condensed horizons in the Jurassic of western India: their significance for basin analysis. J. Geol. Soc. Lond. 149, 313–331.
Fürsich, F.T., Pandey, D.K., Callomon, J.H., Jaitly, A.K., Singh, I.B., 2001. Marker beds in the Jurassic of the Kachchh Basin, Western India, their depositional environment and sequence stratigraphic significance. J. Palaeontol. Soc. India 46, 173–198.
Fürsich, F.T., Oschmann, W., Pandey, D.K., Jaitly, A.K., Singh, I.B., Liu, C., 2004. Paleoecology of Middle to Lower–Upper Jurassic macrofaunas of the Kachchh Basin, Western India: an overview. J. Palaeontol. Soc. India 49, 1–26.
Fürsich, F.T., Singh, I.B., Joachimski, M., Krumm, S., Schlirf, M., Schlirf, S., 2005. Palaeoclimate reconstructions of the Middle Jurassic of Kachchh (western India), an integrated approach based on palaeoecological, oxygen isotopic, and clay mineralogical data. Palaeogeogr. Palaeoclimatol. Palaeoecol. 217, 289–309.
Fürsich, F.T., Alberti, M., Pandey, D.K., 2013. Stratigraphy and Palaeoenvironments of the Jurassic Rocks of Kachchh – Field Guide. Beringeria, Special Issue. 7. pp. 1–174.
Gaillard, C., 1983. Les biohermes à spongiaires et leur environment dans l'Oxfordian du Jura méridional. (Doc. Lab. Géol. Lyon 90 515 pp.).
Gambacorta, G., Trincianti, E., Torricelli, S., 2016. Anoxia controlled by relative sea–level changes: an example from the Mississippian Barnett Shale Formation. Palaeogeogr. Palaeoclimatol. Palaeoecol. 459, 306–320.
Gaur, K.N., Talib, A., 2009. Middle–Upper Jurassic foraminifera from Jumara Hills, Kutch, India. Rev. Micropaleontol. 52, 227–248.
Gómez, J.J., Canales, M.L., Ureta, S., Goy, A., 2009. Palaeoclimatic and biotic changes during the Aalenian (Middle Jurassic) at the southern Laurasian Seaway (Basque–Cantabrian Basin, northern Spain). Palaeogeogr. Palaeoclimatol. Palaeoecol. 275, 14–27.
Gradstein, F.M., 1978. Jurassic Grand Banks foraminifera. J. Foraminifer. Res. 8, 97–109.
Gradstein, F.M., 1983. Paleoecology and stratigraphy of Jurassic abyssal foraminifera in the Blake–Bahama Basin, Deep Sea Drilling Project Site 534. In: Sheridan, R.E., Gradstein, F.M. (Eds.), Initial Reports, Deep Sea Drilling Project. 76. pp. 537–560.
Grunert, P., Soliman, A., Ćorić, S., Roetzel, R., Harzhauser, M., Piller, W.E., 2012. Facies development along the tide–influenced shelf of the Burdigalian Seaway: an example from the Ottnangian stratotype (early Miocene, middle Burdigalian). Mar. Micropaleontol. 84–85, 14–36.
Hallam, A., Grose, J.A., Ruffell, A.H., 1991. Palaeoclimatic significance of changes in clay mineralogy across the Jurassic–cretaceous boundary in England and France. Palaeogeogr. Palaeoclimatol. Palaeoecol. 81 (3–4), 173–187.
Hammer, Ø., Harper, D.A.T., Ryan, P.D., 2001. PAST: paleontological statistics software package for education and data analysis. Palaeontol. Electron. 4, 1–9.
Haq, B.U., 2018. Jurassic sea–level variations, a reappraisal. GSA Today 28, 1. https://doi.org/10.1130/GSATG359A.
Henriques, M.H., Canales, M.L., 2013. Ammonite–benthic foraminifera turnovers across the Lower–Middle Jurassic transition in the Lusitanian Basin (Portugal). Geobios 46, 395–408.
Hess, S., Kuhnt, W., 1996. Deep–sea benthonic foraminiferal recolonization of the 1991 Mt. Pinatubo ash layer in the South China Sea. Mar. Micropaleontol. 30, 1–27.
Hesselbo, S.P., Deconinck, J.F., Huggett, J.M., Morgans–Bell, H.S., 2009. Late Jurassic palaeoclimatic change from clay mineralogy and gamma–ray spectrometry of the Kimmeridge Clay, Dorset, UK. J. Geol. Soc. Lond. 166, 1123–1133.
Hughes, G.W., 2004. Middle to Upper Jurassic Saudi Arabian carbonate petroleum reservoirs, biostratigraphy, micropalaeontology and palaeoenvironments. GeoArabia 9, 79–114.
Jain, S., 1996. Biostratigraphical and Paleoecological Studies of Middle Jurassic (Upper Bathonian–Lower Callovian) Beds Exposed in Jumara Dome, Kachchh, Western India. (Unpublished Thesis, 202 pp.).
Jain, S., 2014. A new early Middle Bathonian Arkelli Chronozone in Kachchh, western India (South Tethys). Zitteliana A 54, 91–146.
Jain, S., Pandey, D.K., 2000. Middle Jurassic Ammonite Biozonation in Kachchh, western India. Bull. Indian Geol. Assoc. 33, 1–12.
Jain, S., Callomon, J.H., Pandey, D.K., 1996. On the earliest known occurrence of the Middle Jurassic ammonite genus Reineckeia in the Upper Bathonian of Jumara, Kachchh, Western India. Paläontol. Z. 70, 129–143.
Jain, S., Collins, L.S., Hayek, L.A.-C., 2007. Relationship of benthic foraminiferal diversity to paleoproductivity in the neogene of the Caribbean Deep–Sea. Palaeogeogr. Palaeoclimatol. Palaeoecol. 225, 223–245.
Johnson, B., 1976. Ecological ranges of selected Toarcian and Domerian (Jurassic) foraminiferal species from Wales. In: Schafer, C.T., Pelletier, B.R. (Eds.), Proceedings of the 1st International Symposium on Benthonic Foraminifera of Continental Margins. 1. Maritime Sediments Special Publication, pp. 545–556.
Jones, R.W., Charnock, M.A., 1985. "Morphogroups" of agglutinating foraminifera: their life position, feeding habits and potential applicability in (paleo)ecological studies. Rev. Paléobiol. 4, 311–320.
Jorissen, F.J., de Stigter, H.C., Widmark, J.G.V., 1995. A conceptual model explaining benthic foraminiferal microhabitats. Mar. Micropaleontol. 26 (1–4), 3–15.
Kaiho, K., 1991. Global changes of Paleogene aerobic/anaerobic benthic foraminifera and deep–sea circulation. Palaeogeogr. Palaeoclimatol. Palaeoecol. 83, 65–85.
Kaiho, K., 1994. Benthic foraminiferal dissolved-oxygen index and dissolved-oxygen levels in the modern ocean. Geology 22, 719–722.
Kaminski, M.A., Gradstein, F.M., Berggren, W.A., Geroch, S., Beckmann, J.P., 1988. Agglutinated foraminiferal assemblages from Trinidad, taxonomy, stratigraphy and paleobathymetry. Abh. Geol. Bundesanst. 41, 155–228.
Kaminski, M.A., Boersma, A., Tyszka, J., Holbourn, A.E.L., 1995. Response of deep–water agglutinated foraminifera to dysoxlc conditions in the California Borderland Basins. In: Kaminski, M.A., Geroch, S., Gasinski, M.A. (Eds.), Proceedings of the Fourth International Workshop on Agglutinated Foraminifera. Grzybowski Foundation Special Publication 3. pp. 131–140.
Kottachchi, N., Schröder–Adams, C.J., Haggart, J.W., Tipper, H.W., 2002. Jurassic Foraminifera from the Queen Charlotte Islands, British Columbia, Canada, biostratigraphy, paleoenvironments and paleogeographic implications. Palaeogeogr. Palaeoclimatol. Palaeoecol. 180, 93–127.
Koutsoukos, E.A.M., Leary, P.N., Hart, M.B., 1990. Latest Cenomanian–earliest Turonian low oxygen tolerant benthonic foraminifera: a case study from the Sergipe basin (N.E. Brazil) and the western Anglo–Paris basin (southern England). Palaeogeogr. Palaeoclimatol. Palaeoecol. 77, 145–177.
Krautter, M., 1997. Aspekte zur paläökologie postpaläaozoischer Kieselschämme. Profil 11, 199–324.
Krautter, M., 1998. Ecology of siliceous sponges – Application to the environmental interpretation of the Upper Jurassic sponge facies (Oxfordian) from Spain. Cuader. Geol. Ibérica 24, 223–239.
Krishna, J., Ojha, J.R., 2000. The intra-basinal correlations in the Middle Jurassic Callovian stage of Kachchh (Gujarat) and ammonoid–foraminifer integration. Geophytology 28, 101–120.
Langer, M.R., 1993. Epiphytic foraminifera. Mar. Micropaleontol. 20, 235–265.
Le Galvez, Y., 1958. Les foraminifères de la mer Celtique. Rev. Trav. Inst. Pêches Marit. 22, 147–194.
Leckie, M., Olson, H.C., 2003. Foraminifera as proxies for sea–level change on siliciclastic margins. In, Micropaleontologic Proxies for Sea–Level Change and Stratigraphic Discontinuities. SEPM Spec. Publ. 75, 5–19.
Malchus, N., Steuber, T., 2002. Stable isotope records (O, C) of Jurassic aragonitic shells from England and NW Poland; palaeoecologic and palaeoenvironmental implications. Geobios 35, 29–39.
Meyer, M., 2000. Le complexe récifal Kimméridgien–Tithonien du Jura meridional interne (France), évolution multifactorielle, stratigraphie et tectonique. Terre Environ. 24 (179 pp.).
Morris, P.H., 1982. Distribution and palaeoecology of Middle Jurassic Foraminifera from the Lower Inferior Oolite of the Cotswolds. Palaeogeogr. Palaeoclimatol. Palaeoecol. 3l7 (2–4), 319–347.
Morris, P.H., Coleman, B.E., 1989. In: Jenkins, D.G., Murray, J.W. (Eds.), Stratigraphical Atlas of Fossil Foraminifera, 2nd edition. The Aalenian to Callovian (Middle Jurassic). pp. 189–236.
Muller Jr., F.L., 1990. The Paleoecology of the Liassic Benthic Foraminifera of Great Britain. Unpublished Ph.D. Thesis, Graduate School – New Brunswick. Rutgers, The State University of New Jersey, pp. 310.
Murray, J.W., 1991. Ecology and Paleoecology of Benthic Foraminifera. Longman, Harlow, pp. 397.
Nagy, J., 1992. Environmental significance of foraminiferal morphogroups in Jurassic North Sea deltas. Palaeogeogr. Palaeoclimatol. Palaeoecol. 95, 111–134.
Nagy, J., Grandstein, F.M., Kaminski, M.A., Holbourn, A.E., 1995. Foraminiferal morphogroups, paleoenvironments and new taxa from Jurassic to cretaceous strata of Thakkhola, Nepal. In: Grzybowski Foundation Special Publication. 3. pp. 181–209.
Neyman, A.A., 1967. Limits to the application of the trophic group concept in benthic studies. Oceanol. Acad. Sci. USSR 7, 149–155.
Olóriz, F., Reolid, M., Rodríguez-Tovar, F.J., 2002. Fossil assemblages, lithofacies and taphofacies for interpreting depositional dynamics in epicontinental Oxfordian of Prebetic Zone, Betic Cordillera, southern Spain. Palaeogeogr. Palaeoclimatol. Palaeoecol. 185, 53–75.
Olóriz, F., Reolid, M., Rodríguez–Tovar, F.J., 2003. Palaeogeographic and stratigraphic distribution of mid–late Oxfordian foraminiferal assemblages in the Prebetic Zone (Betic Cordillera, Southern Spain). Geobios 36, 733–747.
Pandey, J., Dave, A., 1993. Studies in Mesozoic Foraminifera and chronostratigraphy of Western Kutch, Gujarat. Palaeontogr. Indica 1, 1–221.
Rai, J., Jain, S., 2013. Pliensbachian nannofossils from Kachchh: implications on the earliest Jurassic transgressive event on the Western Indian margin. Zitteliana A 53, 105–120.
Reolid, M., 2008. Taphonomic features of *Lenticulina* as a tool for paleoenvironmental interpretation of midshelf deposits of the Upper Jurassic (Prebetic Zone, Southern Spain). Palaios 23, 482–494.
Reolid, M., Martínez-Ruiz, F., 2012. Comparison of benthic foraminifera and geochemical proxies in shelf deposits from the Upper Jurassic of the Prebetic (southern Spain). J. Iber. Geol. 38 (2), 449–465.
Reolid, M., Rodríguez-Tovar, F.J., Nagy, J., Olóriz, F., 2008a. Benthic foraminiferal

morphogroups of mid to outer shelf environments of the late Jurassic (Prebetic Zone, southern Spain): Characterization of biofacies and environmental significance. Palaeogeogr. Palaeoclimatol. Palaeoecol. 261, 280–299.
Reolid, M., Nagy, J., Rodríguez – Tovar, F.J., Olóriz, F., 2008b. Foraminiferal assemblages as palaeoenvironmental bioindicators in late Jurassic epicontinental platforms, relation with trophic conditions. Acta Palaeontol. Pol. 53, 705–722.
Reolid, M., Sebane, A., Rodríguez-Tovar, F.J., Marok, A., 2012. Foraminiferal morphogroups as a tool to approach the Toarcian Anoxic Event in the Western Saharan Atlas (Algeria). Palaeogeography, Palaeoclimatology, Palaeoecology 323–325, 87–99.
Reolid, M., Chakiri, S., Bejjaji, Z., 2013. Adaptative strategies of the Toarcian benthic foraminiferal assemblages from the Middle Atlas (Morocco): palaeoecological implications. J. Afr. Earth Sci. 84, 1–12.
Reuter, M., Piller, W.E., Brandano, M., 2013. Fossil psammobiontic sponges and their foraminiferal residents, central Apennines, Italy. Palaios 28, 614–622.
Riegraf, W., 1985. Mikrofauna, Biostratigraphie und Fazies im unteren Toarcium Südwestdeutschlands und Vergleiche mit benachbarten Gebieten. Tübinger Mikropaläontologische Mitteilungen 3, 1–232.
Riegraf, W., Luterbacher, H., 1989. Upper Jurassic foraminifers of the North and South Atlantic Deep Sea Drilling Project Leg 1–79. Geol. Rundsch. 78, 999–1045.
Rita, P., Reolid, M., Duarte, L.V., 2016. Benthic foraminiferal assemblages record major environmental perturbations during the late Pliensbachian–early Toarcian interval in the Peniche GSSP, Portugal. Palaeogeogr. Palaeoclimatol. Palaeoecol. 454, 267–281.
Sagasti, G., Ballent, S., 2002. Microfaunal features of a marine transgression: the Agrio Formation (lower cretaceous), Neuquen Basin, Argentina. Geobios 35 (6), 721–734.
Samson, Y., 2001. Foraminifères et reconstitution des variations bathymétriques, exemple du Kimméridgien de la région du Havre (Seine–Maritime, Normandie, France). Rev. Micropaleontol. 44, 59–91.
Sjoerdsma, P.G., Van der Zwaan, G.J., 1992. Simulating the effect of changing organic flux and oxygen content on the distribution of benthic foraminifera. Mar. Micropaleontol. 19, 163–180.
Smolen, J., 2012. Faunal dynamics of foraminiferal assemblages in the Bathonian (Middle Jurassic); Ore–bearing Clays at Geznaszyn, Kraków–Silesia Homocline, Poland. Acta Geol. Pol. 62 (3), 403–419.
Springer, Rasmussen, J.A., Stemmerik, L., 2016. Distribution and significance of foraminiferal biofacies on an aphotic Danian bryozoan mound, Karlstrup, Denmark. Bull. Geol. Soc. Den. 64, 57–67.
Stam, B., 1985. Quantitative analysis of Middle and late Jurassic foraminifera from Portugal and its implications for the Grand Banks of Newfoundland. Utrecht Micropaleontol. Bull. 34, 1–168.
Talib, A., Gaur, K.N., 2005. Foraminiferal palaeoecology, microfacies and palaeo–environment of Middle–Upper Jurassic sequence, Jumara Hills, western Kutch, Gujarat. Ind. J. Petrol. Geol. 14, 9–21.
Theodoridis, S., Koutroumbas, T., 2008. Pattern Recognition. Academic Press 984 pp.
Tyszka, J., 1994a. Paleoenvironmental implications from ichnological and microfaunal analyses of Bajocian spotty carbonates, Pieniny Klippen Belt, Polish Carpathians. Palaios 9, 175–187.
Tyszka, J., 1994b. Response of Middle Jurassic benthic foraminiferal morphogroups to dysoxic/anoxic conditions in the Pieniny Klippen Basin, Polish Carpathians. Palaeogeogr. Palaeoclimatol. Palaeoecol. 110, 55–81.
Tyszka, J., 2001. Microfossil Assemblages as Bathymetric Indicators of the Toarcian/Aalenian “Fleckenmergel”–Facies in the Carpathian Pieniny Klippen Belt. Geol. Carpath. 52 (3), 147–158.
Van der Zwaan, G.J., Duijnstee, I.A.P., den Dulk, M., Ernst, S.R., Jannink, N.T., Kouwenhoven, T.J., 1999. Benthic foraminifers: proxies or problems?: a review of paleocological concepts. Earth Sci. Rev. 46, 213–236.